Regulatory and functional aspects of indolic metabolism in plant systemic acquired resistance

Elia Stahl[a,d], Patricia Bellwon[b], Stefan Huber[a], Klaus Schlaeppi[b,e], Friederike Bernsdorff[a], Armelle Vallat-Michel[c], Felix Mauch[b], Jürgen Zeier[a,d,1]

[a] Department of Biology, Heinrich Heine University Düsseldorf, Universitätsstraße 1, D-40225 Düsseldorf, Germany

[b] Plant Biology Section, University of Fribourg, Route Albert Gockel 3, CH-1700 Fribourg, Switzerland

[c] Institut de Chimie, Université de Neuchâtel, Av. Bellevaux 51, CH-2007 Neuchatel, Switzerland

[d] Cluster of Excellence on Plant Sciences (CEPLAS)

[e] Present address: Agroscope Institute for Sustainability Sciences, Reckenholzstrasse 191, CH-8046 Zürich, Switzerland

[1] To whom correspondence should be addressed. E-mail Juergen.Zeier@uni-duesseldorf.de.

tel. 49-211-81-14733, fax 49-211-81-13335.

Running title: Indolic compounds in systemic acquired resistance

Short summary: We investigate regulatory principles of different branches of indolic metabolism during *Arabidopsis thaliana* systemic acquired resistance (SAR) induced with the bacterial pathogen *Pseudomonas syringae*. Upon SAR induction, indol-3-ylmethylamine and indole-3-carboxylic acid are the major accumulating indoles systemically in the shoot. The functional relevance of indolic metabolism for SAR is described, and different resistance phenotypes between soil- and hydroponically-cultured plants defective in indolic metabolism are revealed.

ABSTRACT

Tryptophan-derived, indolic metabolites possess diverse functions in Arabidopsis innate immunity to microbial pathogen infection. Here, we investigate the functional role and regulatory characteristics of indolic metabolism in Arabidopsis systemic acquired resistance (SAR) triggered by the bacterial pathogen *Pseudomonas syringae.* Indolic metabolism is broadly activated in both *P. syringae*-inoculated and in distant, non-inoculated leaves. At inoculation sites, camalexin, indol-3-ylmethylamine (I3A), and indole-3-carboxylic acid (ICA) are the major accumulating compounds, along with about 20 other detected indolics. Camalexin accumulation is positively affected by the transcription factor *MYB122*, and by the cytochrome P450 genes *CYP81F1* and *CYP81F2*. Local I3A production, by contrast, occurs via indole glucosinolate breakdown by pathways dependent and independent of the myrosinase PEN2. Moreover, exogenous application of the defense hormone salicylic acid stimulates I3A generation at the expense of its precursor indol-3-ylmethylglucosinolate (I3M), and the SAR regulator pipecolic acid primes plants for enhanced *P. syringae*-induced activation of distinct branches of indolic metabolism. In uninfected systemic tissue, the metabolic response is more specific and associated with enhanced levels of the indolics I3A, ICA, and indole-3-carbaldehyde (ICC). Systemic indole accumulation fully depends on functional *CYP79B2/3*, *PEN2*, and *MYB34/51/122*, and requires functional SAR signalling. Mutant analyses suggest that systemically elevated indoles are dispensable for SAR directed against *P. syringae* and associated systemic increases of salicylic acid. However, soil-grown but not hydroponically-cultivated *cyp79b2/3* and *pen2* plants, both defective in indolic secondary metabolism, exhibit pre-induced immunity, which abrogates their intrinsic ability to induce SAR.

INTRODUCTION

The immune system of plants is based on a multi-layered arsenal of constitutive and inducible defense strategies (Thordal-Christensen et al., 2003). These involve the action of low molecular weight plant metabolites at different functional levels. Phytoanthicipins are pre-existing plant natural products with antimicrobial activity that can act as resistance determinants of plant species to insufficiently adapted pathogenic microbes (Bednarek and Osbourn, 2009). For instance, antifungal triterpene saponins such as avenacin protect oat plants against root infection by varieties of the fungal pathogen *Gaeumannomyces graminis* that lack saponin-deglycosylating enzymes (Papadopoulou et al., 1999). Phytoalexins, by contrast, are antimicrobial low molecular weight secondary metabolites only produced in the course of a plant-pathogen interaction. The antifungal sorghum deoxyanthocyanidins apigeninidin and luteolinidin, which focally accumulate in response to attempted infection by the fungus *Colletotrichum graminicola* in attacked leaf cells, are classical examples for phytoalexins (Snyder and Nicholson, 1990).

Some plant metabolites act as defensive signals, coordinating the expression of defense-related genes and promoting plant pathogen resistance by regulatory means. The phenolic salicylic acid (SA) is produced from chorismate in response to attack by many microbes and confers disease resistance to many biotrophic and hemibiotrophic pathogens (Nawrath and Métraux, 1999; Wildermuth et al., 2001; Vlot et al., 2009). The biosynthesis of SA is a central part of the inducible defense repertoire of plants that is activated after the perception of common microbial structures, so-called pathogen-associated molecular patterns (PAMPs), or after the recognition of effectors highly specific to particular pathogen isolates (Spoel and Dong, 2012). In contrast to effector-triggered immunity (ETI) that culminates in a localized cell death reaction at sites of pathogen ingress, PAMP-triggered immunity (PTI) is weaker and usually not efficient enough to entirely prohibit infection by adapted pathogens (Jones and Dangl, 2006).

PTI or plant basal resistance can be augmented by biotic and abiotic environmental cues (Singh et al., 2014). A well-known response of plants to biotic stress is systemic acquired resistance (SAR) (Shah and Zeier, 2013; Fu and Dong, 2013). SAR develops after a localized microbial leaf inoculation and provides broad-spectrum resistance to subsequent infection in the whole foliage. SA is an important regulatory metabolite in the SAR process. In *Arabidopsis thaliana*, proper SAR activation requires pathogen-induced, ISOCHORISMATE SYNTHASE1 (ICS1)-mediated SA accumulation (Nawrath and

Métraux, 1999; Wildermuth et al., 2001). Another central SAR regulatory metabolite is the non-protein amino acid pipecolic acid (Pip) (Návarová et al., 2012). In Arabidopsis plants attacked by the bacterial pathogen *Pseudomonas syringae*, Pip and SA accumulate both in inoculated leaves and systemically in leaf tissue distant from initial inoculation. Pip is synthesized from Lys upon pathogen attack by AGD2-LIKE DEFENSE RESPONSE PROTEIN 1 (ALD1) and enhances plant resistance via FLAVIN-DEPENDENT MONOOXYGENASE 1 (FMO1) (Návarová et al., 2012; Zeier, 2013). Both *ALD1* and *FMO1* are indispensable for SAR (Song et al., 2004; Mishina and Zeier, 2006; Návarová et al., 2012). During SAR, elevated Pip levels prime plants for enhanced and effective defense activation upon subsequent pathogen challenge (Návarová et al., 2012; Vogel-Adghough et al., 2013; Bernsdorff et al., 2016).

The significance of Pip in SAR exemplifies that amino acid-related metabolic pathways accomplish integral tasks in the plant immune system (Zeier, 2013). Tryptophan (Trp) catabolism constitutes another important metabolic branch in plant immunity that produces defense-relevant indolic compounds. Trp-derived indolics are particularly prominent in Arabidopsis and other cruciferous plants (Bednarek et al., 2011). The entry reaction into indolic secondary metabolism in Arabidopsis is catalysed by the two cytochrome P450 enzymes CYP79B2 and CYP79B3, which convert Trp into indole-3-acetaldoxime (IAOx) (Zhao et al., 2002). From IAOx, several branches of indolic metabolism diverge, leading to the formation of indole glucosinolates, the phytoalexin camalexin, and a series of other low molecular weight indolics including indole-3-carboxylic acid (ICA) and the phytohormone indole-3-acetic acid (Glawischnig, 2007; Bender and Celenza, 2009; Sonderby et al., 2010; Bednarek, 2012).

Indol-3-ylmethylglucosinolate (I3M) constitutes the major indole glucosinolate in Arabidopsis rosette leaves (Brown et al., 2003). Members of the cytochrome P450 subfamily CYP81F are able to hydroxylate I3M and thereby catalyse the first step in the formation of less-prominently occurring 4- and 1-methoxylated I3M derivatives (Pfalz et al., 2011). Indole glucosinolates can be degraded enzymatically or non-enzymatically to different breakdown products. I3M hydrolysis, for instance, can lead to the formation of indole-3-acetonitrile (IAN) and indole-3-carbinol (I3C) (Kim et al., 2008). Moreover, fungal attack causes conversion of I3M to indol-3-ylmethylamine (I3A) in a *PENETRATION2* (*PEN2*)-dependent manner (Bednarek et al., 2009). *PEN2* encodes an atypical myrosinase that has been initially identified as a critical determinant of Arabidopsis penetration resistance to non-adapted

powdery mildew pathogens (Lipka et al., 2005; Bednarek et al., 2009). It is now established that the indole glucosinolate/PEN2-myrosinase system constitutes an important early defense layer that restricts invasion of Arabidopsis by different non-adapted and adapted fungal and oomycete pathogens (Sanchez-Vallet et al., 2010; Schlaeppi et al., 2010; Consonni et al., 2010; Bednarek, 2012; Hiruma et al., 2013). The biosynthesis of indolic glucosinolates is distinctly regulated by the three MYB-type transcription factors MYB34, MYB51 and MYB122 (Frerigmann and Gigolashvili, 2014).

Another branch of indolic metabolism results in the formation of camalexin, the most prominent phytoalexin in Arabidopsis (Glawischnig, 2007). Camalexin accumulates to high levels in Arabidopsis leaves inoculated with hemibiotrophic *P. syringae* bacteria or nectrotrophic fungi such as *Alternaria brassicola* or *Botrytis cinerea* and exhibits *in vitro* antimicrobial activity (Kliebenstein et al., 2005; Schuhegger et al., 2007). SAR-induced plants are primed for enhanced camalexin biosynthesis through Pip accumulation (Návarová et al., 2012). The *phytoalexin-deficient3* (*pad3*) mutant is defective in camalexin biosynthesis and exhibits increased susceptibility to *A. brassicicola* and *B. cinerea* but not to *P. syringae* infection, indicating that camalexin protects against the former two but not against the latter pathogen (Thomma et al., 1999; Ferrari et al., 2007). The sequential action of indole glucosinolates and camalexin restricts colonisation of Arabidopsis by the hemibiotrophic oomycete *Phytophtora brassicae* (Schlaeppi et al., 2010). The two cytochrome P450 enzymes CYP71A13 and CYP71B15 (alias PAD3) participate in camalexin biosynthesis. *In vitro* biochemical studies indicate that CYP71A13 acts in an earlier step of camalexin biosynthesis and converts IAOx to IAN (Nafisi et al., 2007). PAD3 catalyzes the two final biosynthetic steps from Cys-IAN to camalexin (Schuhegger et al., 2006; Böttcher et al., 2009).

In addition to camalexin, indole-3-carbaldehyde (ICC), ICA and ICA-derivatives are formed in response to pathogen infection or abiotic stress in Arabidopsis roots and leaves (Hagemeier et al., 2001; Bednarek et al., 2005; Böttcher et al., 2009; Iven et al., 2012; Gamir et al., 2012). Besides accumulating in free or glycosylated form, ICA is esterified to cell wall components in pathogen-inoculated tissue (Tan et al., 2004; Forcat et al., 2010). Recently, a model for the biosynthesis of ICC and ICA derivatives, involving ARABIDOPSIS ALDEHYDE OXIDASE1 (AAO1) and CYP71B6, was presented (Böttcher et al., 2014).

In the present work, we investigate the significance and regulatory characteristics of indolic metabolism during the Arabidopsis SAR response. We show that *P. syringae*-induced SAR is accompanied by a strong and broad activation of indolic metabolism in inoculated

leaves and in uninfected, systemic leaves. The local metabolic response includes strong accumulation of camalexin, I3A, and ICA, and enhanced production of about 20 other GC/MS-detectable indolic compounds. Metabolite analyses of indole pathway mutants suggest that besides *CYP71A13* and *PAD3*, the cytochrome P450 *CYP81F1* and *CYP81F2,* and the MYB transcription factor *MYB122* positively regulate camalexin production. Moreover, mutational defects of *CYP71A13, CYP81F1* and *CYP81F2* cause metabolic imbalances that result in over-accumulation of IAN, I3A, and ICA upon bacterial inoculation. Local I3A production proceeds via PEN2-dependent and independent metabolic pathways, and I3A generation from I3M is stimulated by exogenous SA. Similar to camalexin accumulation (Návarová et al., 2012), the pathogen-induced biosynthesis of I3A and ICA is primed by pre-treatment of plants with Pip. In leaves distant from inoculation, the *P. syringae*-induced activation of indolic metabolism results in the accumulation of I3A, ICA, and ICC, indicating that SAR establishment equips plants with increased levels of defense-relevant indolics throughout the foliage. However, mutant analyses argue against a direct functional role for these indolics in general SAR activation. Notably, mutational defects of *CYP79B2/3* and *PEN2*, which weakens pre-invasion immune layers, can lead to a pre-activation of post-invasion defenses in soil-grown plants that increases plant basal resistance and results in an apparent loss of SAR inducibility.

RESULTS

SAR establishment in Arabidopsis is associated with a strong activation of indolic metabolism

A localized leaf inoculation with avirulent or virulent strains of the bacterial pathogen *Pseudomonas syringae* induces systemic acquired resistance in the foliage of Arabidopsis plants (Shah and Zeier, 2013). Two days after inoculation of lower (1°) leaves with the compatible *P. syringae* pv. *maculicola* ES4326 (*Psm*) strain, SAR fully develops in non-treated upper (2°) leaves. This is associated with significant accumulation of the two SAR-regulatory metabolites SA and Pip, and with a massive transcriptional reprogramming in 2° leaves (Návarová et al., 2012; Gruner et al., 2013; Bernsdorff et al., 2016). To investigate a possible role of indolic metabolism in the establishment of SAR, we performed comparative GC/MS-based metabolite analyses of 1° treated leaves and non-treated 2° leaves two days after *Psm* inoculation or mock-control treatment in Arabidopsis wild-type and selected mutant lines.

The precursor amino acid for indolic secondary metabolites, Trp (A) (Fig. 1), significantly accumulates in *Psm*-inoculated leaves of wild-type Col-0 plants (Fig. 2; Návarová et al., 2012). A *cyp79b2 cyp79b3* (*cyp79b2/3*) double knockout mutant is blocked in the production of Trp-derived metabolites such as indole glucosinolates and camalexin (Glawischnig et al., 2004; Böttcher et al., 2009; Bednarek et al., 2009). By GC/MS-profiling, we comparatively analysed metabolic changes in wild-type Col-0 and *cyp79b2/3* in *Psm*-treated 1° leaves compared to mock-treated control leaves. Based on comparative analyses of individual ion chromatograms (m/z between 50 and 300), we identified 22 substances that significantly accumulated in extracts of *Psm*-inoculated Col-0 leaves but not in leaves of *cyp79b2/3*, suggesting that these compounds represent Trp-derived metabolites (Table 1). By comparison of their mass spectra and retention times with those of authentic standards, and by matching of mass spectra with spectra from the NIST library, we were able to identify 9 of these 22 substances. All of them represent 3-substituted indole derivatives (Table 1, Fig. 1).

As expected, the indolic phytoalexin camalexin (B) prominently accumulated in *Psm*-inoculated (1°) leaves of Col-0 at 48 hours post inoculation (hpi) (Table 1, Figs. 1 and 2). Moreover, ICA (D) and, as deduced from its similar mass spectrum, a substance structurally related to ICA (substance #15 in Table 1), were substantially produced in *Psm*-inoculated Col-0 leaves (Table 1, Figs. 1 and 2). Albeit accumulating to lower absolute levels than ICA, the levels of ICC (E), indole-3-carbonitrile (ICN, G), and indole (C) were also significantly increased at sites of bacterial attack (Table 1, Figs. 1 and 2). A comparatively weak but statistically significant enrichment was found for three other compounds, 4-methoxy-indole-3-acetonitrile (I), I3C (J), and tryptophole (K). Further, IAN (H) was present in extracts of Col-0 plants but hardly detectable in extracts of *cyp79b2/3*. IAN levels, however, were not significantly influenced by bacterial attack (Table 1). 12 of the 20 pathogen-induced substances that were designated as indolics by the GC/MS-based profiling analyses could not be structurally identified. However, the mass spectra of 3 of these compounds exhibited close similarity to the spectra of 2-methyl-ICA, 5-hydroxy-ICC, and 5-methoxy-tryptophole (Table 1). Although the unidentified compounds only accumulated to comparatively low absolute levels in Col-0, virtually all of these substances showed a marked relative enrichment in extracts from *Psm*-inoculated compared to extracts from control leaves.

In Arabidopsis leaves inoculated with non-adapted powdery mildew fungi, the indolic amine I3A (Fig. 1, substance F) accumulates at fungal inoculation sites. I3A is a hydrolysis product of I3M (Fig. 1, substance L), the main indole glucosinolate in accession Col-0

(Brown et al., 2003; Bednarek et al., 2009). Due to their hydrophilic nature, I3M and I3A are not analyzable by the GC/MS-based analytical method applied for the above-described indolics. We therefore applied targeted, HPLC-based analysis to determine whether the leaf levels of I3A and I3M would be altered upon bacterial inoculation. Strikingly, *Psm* treatment of plants triggered a very strong increase of I3A levels in inoculated leaves, which came quantitatively close to the induced levels of camalexin at 48 hpi (Fig. 2). Concomitantly, the levels of I3M significantly decreased in leaves inoculated with *Psm*, consistent with a conversion of I3M into I3A upon bacterial attack (Fig. 2).

Our data so far indicate that indolic metabolism is strongly activated in *Psm*-inoculated, 1° leaves in the course of SAR establishment. The accumulating indolics share this feature with various structurally unrelated metabolites, such as branched-chain and aromatic amino acids, Lys, Pip, α-aminoadipic acid, free and glycosylated SA, jasmonic acid, unsaturated fatty acids, abscisic acid, the C16-homoterpene (E,E)-4,8,12-trimethyl-1,3,7,11-tridecatetraene (TMTT), and the phytosterol stigmasterol (Mishina and Zeier, 2007; Attaran et al., 2008; Griebel and Zeier, 2010; Návarová et al., 2012; Gruner et al., 2013). Compared to these massive and broad metabolic alterations at bacterial inoculation sites, metabolic changes in distal, non-infected (2°) Arabidopsis leaves upon SAR induction by *Psm* are rare and have only been described for the critical SAR regulators Pip and SA, but not for the other above-enumerated substances (Návarová et al., 2012). Importantly, from the 23 indolic substances determined to locally accumulate upon *Psm*-inoculation (Table 1, Fig. 2), 3 compounds were found to significantly increase in distal, 2° leaf tissue at 48 hpi: I3A, ICA, and ICC (Fig. 2). On the basis of their systemic accumulation in the foliage upon SAR activation, we hypothesized that I3A, ICA, and ICC could be functionally relevant in the SAR process.

Temporal patterns of indolic metabolite accumulation in inoculated leaves

We next examined the temporal accumulation patterns of the most prominently generated indolics at inoculation sites, camalexin, I3A, and ICA, and compared them to SA accumulation in leaves inoculated with the compatible (virulent) *Psm* strain and the avirulent *Psm avrRpm1* strain expressing the *avrRpm1* avirulence gene (Bisgrove at al., 1994). Leaf samples were thereby analyzed at 6, 10, 24, and 48 hpi (Fig. 3). Between 6 and 24 hpi, the *Psm avrRpm1*-triggered accumulation of the examined indolics was stronger than the *Psm*-induced accumulation, indicating that effector-triggered immune signaling exhibits a strong

influence on early indolic metabolite accumulation. At 48 hpi, the indolics accumulated to highest levels in leaves inoculated with *Psm*, suggesting significant contributions of PAMP-triggered immune signaling for the activation of Trp catabolism at later stages of the compatible Arabidopsis-*P. syringae* interaction (Fig. 3). Moreover, ICA and I3A exhibited a similar accumulation pattern than SA during early interaction stages and started to accumulate before camalexin levels increased (Fig. 3).

Biosynthetic and regulatory aspects of indolic metabolism at sites of bacterial inoculation

Besides CYP79B2/3, several other proteins involved in the biosynthesis and the regulation of indolic metabolism have been characterized (Bednarek et al., 2009; Bender and Celenza, 2009; Sonderby et al., 2010; Böttcher et al., 2014). Previous microarray analyses indicate that several of the genes involved in the indolic pathway are up-regulated upon *Psm* inoculation (Table S1; Wang et al., 2008; Gruner et al., 2013). To get further insights into biosynthetic and regulatory aspects of *P. syringae*-induced indolic metabolism, we compared the accumulation pattern of Trp, I3A, ICA, ICC, and camalexin in *Psm*-inoculated leaves at 48 hpi in wild-type Col-0 and selected mutant lines with defined gene defects in Trp-derived metabolism (Figs. 4 and 5). Notably, in *cyp79b2/3*, Trp levels were elevated under basal conditions and over-produced after pathogen infection, whereas, as outlined before (Tab. 1), the Trp-derived indolics were absent or only faintly produced in this mutant (Fig. 4). The blockage of the first step of Trp catabolism in *cyp79b2/3* therefore results in an over-accumulation of Trp, the precursor amino acid of indolic metabolism, after *P. syringae* infection.

The peroxisome-associated glycosyl hydrolase PENETRATION2 (PEN2) contributes to non-host resistance of Arabidopsis to non-adapted fungal and adapted oomycete pathogens (Lipka et al., 2005; Bednarek et al., 2009; Schlaeppi et al., 2010; Sanchez-Vallet et al., 2010). I3A accumulation in Arabidopsis triggered by powdery mildew fungi is fully dependent on functional PEN2 (Bednarek et al. 2009), and we thus analyzed *P. syringae*-triggerd indolic metabolite accumulation in the *pen2-2* (*pen2*) knockout mutant. I3A accumulation in *Psm*-inoculated leaves was markedly lower than in the wild-type, though a significant increase after bacterial inoculation was still detected in *pen2*. In addition, *Psm*-inoculated *pen2* leaves also exhibited attenuated accumulation of ICA, ICC, and camalexin, and did not show pathogen-induced decreases of I3M (Fig. 4; Fig. S1).

The biosynthesis of indole glucosinolates is regulated by the three MYB-type transcription factors MYB34, MYB51, and MYB122 (Malitsky et al., 2008; Gigolashvili et al., 2009). Whereas MYB51 and MYB122 are up-regulated in *Psm*-inoculated leaves, the expression of MYB34 is reduced upon bacterial inoculation (Table S1). Consistent with the function of the three MYB regulators in indole glucosinolate production, a *myb34 myb51 myb122* triple knockout mutant (*tmyb*) showed strongly reduced basal I3M levels and greatly diminished accumulation of indole glucosinolate-derived I3A in *Psm*-inoculated leaves (Fig. 4; Fig. S1). Further, the *Psm*-triggered generation of ICA, ICC, and camalexin was reduced in *tmyb* plants, albeit not to the same extent as I3A production. A similar trend was observed for a *myb51 my122* double mutant (Fig. S2A). Analyses of single MYB knockout mutants indicated that *MYB51* provides the strongest contribution to *Psm*-induced I3A generation, whereas *MYB122* most pronouncedly affects camalexin biosynthesis (Fig. 4). This suggests distinct regulation of different branches of indolic metabolism in *P. syringae*-inoculated leaves. From the overall patterns of metabolite accumulation in the different mutant plants, it appears that ICA and ICC production is closely coordinated, and that the biosynthesis of ICA (ICC), I3A, and camalexin involve distinctive regulatory mechanisms (Fig. 4).

We next examined how defects in camalexin biosynthesis would affect the generation of different indolics in *Psm*-inoculated leaves. The camalexin biosynthesis genes *CYP71A13* and *PAD3* (alias *CYP71B15*) are strongly up-regulated in *Psm*-inoculated leaves (Table S1; Zhou et al., 1999; Nafisi et al., 2007). Whereas PAD3 was shown to catalyze the final steps in camalexin biosynthesis (Schuhegger et al., 2006; Böttcher et al., 2009), biochemical characterization of recombinant CYP71A13 suggests that it is involved in an earlier step in which IAOx is converted to IAN (Nafisi et al., 2007). Consistent with the function of CYP71A13 and PAD3 in camalexin biosynthesis, camalexin accumulation was low or completely absent in *Psm*-inoculated leaves of *cyp71A13-1* (*cyp71A13*) and *pad3-1* (*pad3*) mutant plants, respectively (Fig. 5A). In both mutants, this was accompanied with a strong over-accumulation of IAN, a camalexin pathway intermediate that did not or only slightly accumulate in the wild-type (Fig. 5B). This finding is consistent with the reported function of PAD3 downstream of IAN generation (Böttcher et al., 2009), as blockage of a particular metabolic pathway can result in precursor accumulation. However, since CYP71A13 is reported to catalyze IAOx to IAN conversion (Nafisi et al., 2007), over-accumulation of IAN in *cyp71A13* knockout plants is not readily comprehensible with the currently proposed schemes for camalexin biosynthesis (Geu-Flores et al., 2011; Su et al., 2011). Moreover, the

cyp71A13 but not *pad3* mutant plants also exhibited *Psm*-induced over-accumulation of I3A and ICA (Fig. 5C, D).

Another gene strongly up-regulated in *Psm*-inoculated leaves is *CYP81F1*, one out of four CYP81F gene family members. Transcript levels of the other three members are only slightly (*CYP81F2*) or not (*CYP81F3* and *CYP81F4*) affected by *Psm* inoculation (Table S1). Transient expression assays in *Nicotiana benthamiana* using individual CYP81F isoforms indicate that all four members are capable of hydroxylating I3M to 1- and/or 4-hydroxyindole glucosinolates, which are subsequently methylated in planta (Pfalz et al., 2011). Consistently, Bednarek and colleagues have shown that *CYP81F2* is essential for the powdery mildew-induced accumulation of 4-methoxyindol-3-ylmethylglucosinolate (Bednarek et al., 2009). Surprisingly, both a *cyp81f1* and a *cyp81f2* knockout line showed strongly reduced accumulation of camalexin in *Psm*-inoculated leaves (Fig. 5A). Moreover, as in *cyp71A13*, the reduced camalexin production was associated with a marked over-accumulation of IAN, I3A, and ICA in both *cyp81f1* and *cyp81f2* (Fig. 5B-D). Further, opposing to Col-0 and *pad3*, bacterial attack did not result in decreased levels of the indole glucosinolate I3M in *cyp81f1*, *cyp81f2*, and *cyp71A13* (Fig. S1). Therefore, defects in the two *CYP81F* isoforms and in *CYP71A13* have severe impact on the accumulation of metabolites originating from different branches of indolic metabolism.

The immune regulator salicylic acid is synthesized in *P. syringae*-inoculated Arabidopsis leaves and coordinates the activation of different defense pathways (Vlot et al., 2009). We investigated the impact of exogenously supplied SA on the induction of indolic metabolism, both alone and in combination with a *Psm* challenge (Fig. 6A). For this purpose, leaves of Col-0 plants were infiltrated with 0.5 mM SA, and 4 hours later, the same leaves were infiltrated with mock-solution, a *Psm* suspension, or not treated again. Leaf samples were harvested at 10, 24, and 48 h after the second treatment. SA treatment alone was sufficient to trigger about 5-fold increases in the levels of I3A, and this was apparent for all the time points under investigation and accompanied with decreases in the levels of the precursor glucosinolate I3M (Fig. 6A). Moreover, a *Psm* challenge following SA-pretreatment resulted in significantly stronger increases of I3A than *Psm* challenge alone at 10 hpi. This effect was levelled out at later time points after bacterial challenge (Fig. 6A). Camalexin levels were also increased by exogenous SA alone, although this effect was quantitatively small and only observable late after SA application (from day 1 after treatment onwards). In addition, an SA pre-treatment did not augment the *Psm*-induced camalexin

accumulation (Fig. 6A). Exogenous SA had also no significant effect on basal and *Psm*-induced ICA levels until 24 h after bacterial inoculation (Fig. S3). However, the *Psm*-triggered accumulation of ICA, I3A, and camalexin was lower in SA-pretreated plants at the latest time point after inoculation (48 hpi; Fig. 6A, Fig. S3). This might be related with the strong resistance increase induced by exogenous SA and a consequential significant attenuation of bacterial growth at later infection stages (Fig. S4D), resulting in a considerable lower pathogen stimulus during later stages of the bacterial challenge.

The previous analysis revealed a remarkable effect of the defense hormone SA on indolic metabolism – it promotes I3A generation at the expense of its precursor I3M (Fig. 6A). Pipecolic acid, another immune and SAR regulatory metabolite, also affects the indole pathway, since it is able to prime Arabidopsis plants for enhanced camalexin accumulation (Návarová et al., 2012). Interestingly, pre-treatments of plants with Pip also resulted in a significantly stronger *Psm*-induced generation of I3A and ICA in leaves (Fig. 6B). The primed *Psm*-induced generation of I3A in the presence of elevated Pip was not associated with a stronger pathogen-triggered decrease of I3M, indicating that Pip stimulates I3A generation by general pathway activation rather than by specifically promoting I3M to I3A conversion (Fig. 6B). Pip treatment without subsequent pathogen challenge had no marked effect on I3A or ICA levels (Fig. 6B). Together, these analyses and our previous findings indicate that Pip primes the *P. syringae*-induced activation of several distinct branches of indolic metabolism in Arabidopsis (Fig. 6B; Návarová et al., 2012).

Systemic accumulation of I3A, ICA, and ICC is dependent on *CYP79B2/3, PEN2, MYB34/51* and requires functional SAR signaling

We next examined the genetic components required for the specific accumulation of I3A, ICA, and ICC in systemic, non-inoculated leaf tissue upon SAR induction. Unlike wild-type plants, *cyp79b2/3*, *pen2*, and *tmyb* mutant plants completely lacked the accumulation of I3A, ICA, and ICC in 2° leaves upon 1° leaf-inoculation (Fig. 7). In addition, systemic accumulation of the three indolics was reduced in *myb34* and *myb51* single mutant and in *myb51 myb122* double mutant plants, whereas *cyp71A13* and *myb122* showed wild-type-like accumulation patterns (Fig. 7; Fig. S2B). Thus, the systemic accumulation of indolic metabolites in Arabidopsis fully depends on functional CYP79B2/3, PEN2, and on the combined action of the three myb factors, in particular MYB34 and MYB51. A notable difference between local and systemic accumulation of indole derivatives relies in the fact

that they accumulate in a partially PEN2-independent manner in 1° leaves, whereas they fully require PEN2 to accumulate in 2° leaves.

We then addressed the question as to whether the systemic accumulation of I3A, ICA, and ICC would be functionally relevant for the SAR response. To tackle this issue, we first examined whether the systemic increase of indolics would be associated with the ability of plants to induce SAR. Two indispensable SAR players are Arabidopsis ALD1 and FMO1, which are required for the biosynthesis and signal transduction of the SAR regulator pipecolic acid, respectively (Návarová et al., 2012). In SAR-defective *ald1* and *fmo1* mutants (Song et al., 2004; Mishina and Zeier, 2006; Bernsdorff et al., 2016), the systemic accumulation of the indolics was fully absent (Fig. 8A). In contrast, I3A, ICA, and ICC accumulated in inoculated leaves of *ald1* and *fmo1* to at least the same levels than in inoculated Col-0 leaves (Fig. 7B), indicating that Pip signaling is required for the systemic but not the local production of the indolics.

Two other important SAR components are ICS1/SID2, which is necessary for the pathogen-induced accumulation of SA (Nawrath and Métraux, 1999; Wildermuth et al., 2001), and NON-EXPRESSOR OF PATHOGENESIS-RELATED GENES1 (NPR1), a transcriptional co-activator that acts downstream of SA and has been identified as a bona fide SA receptor (Wu et al., 2012; Fu and Dong, 2013). Although SA-deficient *sid2-1* (*sid2*) mutants are strongly impaired in their ability to induce SAR, recent experiments in our laboratory indicate that a modest residual SAR response takes place in *Psm*-inoculated *sid2* (Bernsdorff et al., 2016). Consistent with this, the *Psm*-induced systemic accumulation of I3A, ICA, and ICC was markedly reduced but not fully absent in *sid2* (Fig. 8A). Moreover, *npr1-2* (*npr1*) mutant plants, which suffer from a total loss of *Psm*-triggered SAR (Mishina and Zeier, 2006; Attaran et al., 2009; Návarová et al., 2012), completely fail to accumulate indolic compounds in 2° leaf tissue (Fig. 8A). In *Psm*-inoculated *sid2* and *npr1* leaves, by contrast, the accumulation of ICA and ICC was not impaired. However, a small but significant reduction of I3A accumulation was detected in both *sid2* and *npr1* (Fig. 8B), confirming our conclusions from SA feeding experiments that SA positively regulates *Psm*-induced I3A generation (Fig. 8B). Together, the compromised accumulation of I3A, ICA, and ICC in distal leaves of *ald1*, *fmo1*, *sid2*, and *npr1* indicates that systemic activation of indolic metabolism after *Psm* inoculation requires functional SAR signaling.

Pre-induced immunity of soil-grown *cyp79b2/3* and *pen2* plants mask their intrinsic ability for SAR establishment

The absence of *Psm*-induced systemic accumulation of I3A, ICA, and ICC in *cyp79b2/3*, *pen2* and *tmyb* mutant plants allowed us to directly test their functional relevance in the SAR process. Therefore, we inoculated soil-grown plants with *Psm* in lower 1° leaves to induce SAR or performed a control treatment by infiltrating 10 mM $MgCl_2$. 48 h later, upper 2° leaves of both induced and control plants were challenge-inoculated with *Psm*, and bacterial growth in 2° leaves was assessed three days after the challenge inoculation (Mishina and Zeier, 2007). Wild-type Col-0 plants showed a strong and highly reproducible SAR response, as bacterial multiplication in challenge-inoculated 2° leaves was generally attenuated by 20- to 50-fold as a consequence of the 1°-*Psm*-treatment (Fig. 9A). The situation for *cyp79b2/3* and *pen2* plants was different, because mock-treated plants of these mutants generally exhibited a higher resistance than mock-control plants from the wild-type. The 1° *Psm*-treatment in these lines either failed to induce a significant SAR response or only had a comparatively weak resistance-inducing effect. A typical experimental outcome is shown in Fig. 9A, although the amount of pre-induced resistance in *cyp79b2/3* and *pen2* as well as the degree of the apparently weakened SAR effect in these mutants showed some variation between experiments. We then compared basal resistance to *Psm* on naïve, not previously treated Col-0, *cyp79b2/3*, and *pen2* plants and confirmed the elevated resistance phenotype of soil-grown *cyp79b2/3* and *pen2* (Fig. 9B).

Because of the varying degree of pre-induced resistance in *cyp79b2/3* and *pen2*, we reasoned that variations of resistance-inducing environmental cues during plant growth rather than direct regulatory effects of indolic metabolites might underlie the observed SAR attenuation. When plants were grown in hydroponic culture rather than in soil, the differences in basal resistance between Col-0, *cyp79b2/3*, and *pen2* were virtually absent (Fig. 9B). Notably, the strongly diminished induction of growth-related resistance in hydroponically cultivated *cyp79b2/3* and *pen2* plants was associated with the ability to establish a strong and reproducible SAR response in these mutants (Fig. 9A). This difference between soil- and hydroponically grown plants also got apparent when basal and systemically induced levels of SA were determined. Soil-grown control plants of *cyp79b2/3* and *pen2* contained elevated basal SA levels compared to soil grown wild-type plants (Fig. 9C). They also failed to increase SA levels in 2° leaves upon 1° leaf-inoculation, a characteristic SAR response that is stably observed in wild-type Col-0 plants (Fig. 9C). In contrast to soil-grown plants,

hydroponically cultivated *cyp79b2/3* and *pen2* plants exhibited small or no elevated basal levels of SA, respectively, and systemic SA levels increased to similar levels than in the wild-type upon SAR induction by *Psm* (Fig. 9C). This again indicates that cultivation-dependent resistance induction of *cyp79b2/3* and *pen2* plants alleviate their ability to systemically respond to bacterial inoculation.

Similar to *cyp79b2/3* and *pen2*, *tmyb* mutant plants lacked the systemic elevation of I3A, ICA, and ICC upon *Psm* inoculation, and *myb34, myb51*, and *myb51myb122* showed a markedly attenuated but not fully compromised accumulation of the indolics (Fig. 7; Fig. S2B). Compared to the wild-type, soil-grown *myb34*, *myb51*, *myb51 myb 122*, and *tmyb* plants also exhibited a moderately elevated basal resistance to *Psm*, but this resistance phenotype was markedly less pronounced than the strong phenotype of soil-grown *cyp79b2/3* and *pen2* (Fig. 10). Moreover, all the *myb* mutants were able to increase resistance of 2° leaves to *Psm* in response to a 1° bacterial inoculation to the same extent as Col-0 plants, indicating normal SAR induction in these lines (Fig. 10). SAR establishment in the *myb* lines was also associated with a significant increase of SA levels in 2° leaves (Fig. S5). These findings and the overall SAR data on *cyp79b2/3* and *pen2* indicate that the systemic elevation of I3A, ICA, and ICC observed upon bacterial attack are not crucial for the establishment of SAR in Arabidopsis.

Exogenous application of indole-3-carboxylic acid does not lead to a major resistance increase to *Psm* infection

We have shown previously that exogenous feeding of Arabidopsis or tobacco plants with physiological doses (10 µmol) of the SAR regulator Pip, which systemically accumulates in the plant, substantially increases basal resistance to *P. syringae* (Návarová et al., 2012; Vogel-Adghough et al., 2013; Bernsdorff et al., 2016). Analogously, we investigated whether exogenous application of ICA, one of the systemically accumulating indolics that is commercially available, would elevate resistance of Arabidopsis plants to *Psm* infection. For that, we applied 10 µmol of exogenous ICA to pots of individual Arabidopsis plants and challenge-inoculated leaves one day later with *Psm* (Návarová et al., 2012). In one out of several independent experiments, ICA slightly increased resistance of plants to a subsequent *Psm* challenge in a significant manner, but this increase was low when directly compared to resistance induction by exogenous Pip (Fig. S4A). In the remaining experiments, exogenous ICA failed to induce resistance of Col-0 plants to *Psm* in a statistically significant

manner (Fig. S4B, C). In addition to Col-0, we also employed plants with defects in SAR and/or basal resistance in this assay (Fig. S4C). The mutants included knockout lines of the two key immune regulatory genes *PHYTOALEXIN-DEFICIENT4 (PAD4)* and *NPR1* (Feys et al., 2001; Fu and Dong, 2013). Both *pad4-1* (*pad4*) and *npr1* knockout lines exhibited significantly decreased basal resistance to *Psm* than Col-0 plants, and ICA treatment resulted in a small but significant resistance increase in these mutants which corresponded to a two-fold reduction of bacterial growth at 3 dpi (Fig. S4C). In addition to soil feeding, we also syringe-infiltrated leaves of Col-0 plants with 0.5 mM ICA or SA solutions, challenged-inoculated the same leaves 4 h later with *Psm*, and scored bacterial growth three days later. Whereas SA pre-treatment strongly induced resistance to *Psm*, ICA pre-treatment had no effect (Fig. S4D). Together, the ICA feeding experiments support above-described genetic studies which indicate that ICA is not a critical regulator of SAR and basal immunity to *Psm*. However, ICA seems to moderately contribute to *Psm* resistance if major immune signaling pathways are dysfunctional.

DISCUSSION

Trp catabolism in Arabidopsis proceeds via the cytochrome P450s CYP79B2 and CYP79B3 and diverges into different metabolic branches, leading to the synthesis of indole glucosinolates and their breakdown products, camalexin biosynthesis , and the formation of a series of other low molecular weight indolics such ICA (Fig. 11A; Glawischnig, 2007; Bender and Celenza, 2009; Sonderby et al., 2010; Bednarek, 2012). Previous studies have demonstrated crucial roles of Trp-derived indolics in Arabidopsis immunity against herbivores and a diverse range of microbial pathogens (Glawischnig, 2007; Kim et al., 2008; Bednarek, 2012). In this study, we show that Trp-derived metabolism is broadly activated in Arabidopsis after inoculation with the hemi-biotrophic, SAR-inducing bacterial pathogen *Pseudomonas syringae* pv. *maculicola*, both at sites of bacterial attack (Fig. 11A) and in leaves distant from inoculation. Using Arabidopsis lines defective in defined biochemical or regulatory steps of Trp-derived secondary metabolism, we have investigated regulatory aspects of *P. syringae*-induced indolic metabolism and its functional significance for SAR.

Activation and regulatory aspects of Trp-derived metabolism in *P. syringae*–inoculated leaves

The induction of indolic metabolism in *Psm*-inoculated Col-0 leaves involves, besides a massive production of the phytoalexin camalexin (Tsuji et al., 1992; Glazebrook and Ausubel, 1994; Zhao and Last, 1996), a similarly strong accumulation of the indole glucosinolate breakdown product I3A, markedly enhanced production of ICA, ICC, ICN, I3C, tryptophol, and indole, and the formation of several other, not yet entirely identified indolics (Fig. 1; Fig. 11A). These metabolites are not or only in traces detectable in the *cyp79b2/3* double mutant (Table 1; Figs. 2, 4, 11A). Enhanced de novo synthesis of the precursor amino acid Trp is an integral part of the *P. syringae*-induced activation of indolic metabolism in Arabidopsis (Fig. 2; Hagemeier et al., 2001; Návarová et al., 2012). The blockage of the first step of Trp catabolism in *cyp79b2/3* results in an over-accumulation of the pathway precursor Trp in leaves under basal conditions and after *P. syringae* infection (Figs. 4, 11A).

Our study approves that camalexin accumulation is restricted to the sites of bacterial attack and does not extend to distal leaves (Fig. 2; Gruner et al., 2013). During the first hours after *P. syringae* inoculation, camalexin production lags behind the synthesis of I3A, ICA, or the phenolic SA in naïve plants (Fig. 3). After SAR establishment, however, plants are primed for a faster induction of camalexin biosynthesis if pathogen challenge occurs again (Návarová et al., 2012). Priming of camalexin biosynthesis requires the accumulation of the SAR regulator Pip, and a feasible mechanism includes partial pre-activation of the biosynthetic pathway at the level of transcription, since *CYP71A13* and *PAD3* but not *CYP79B2/3* are up-regulated systemically in SAR-induced plants (Návarová et al., 2012; Gruner et al., 2013; Table S1). Remarkably, feeding of plants with Pip not only primes plants for enhanced camalexin accumulation (Návarová et al., 2012) but also for a stronger production of two other major *P. syingae*-induced indolics, I3A and ICA (Fig. 6B). Therefore, Pip is able to primes the activation of several distinct branches of inducible indolic metabolism in Arabidopsis (Fig. 11A).

Although camalexin heavily accumulates upon bacterial attack in Arabidopsis leaves, bacterial growth assays with camalexin-deficient *pad3* demonstrate that the phytoalexin is dispensable for the full expression of basal immunity to *P. syringae* (Glazebrook and Ausubel, 1994). By contrast, camalexin is a direct resistance determinant of Arabidopsis to the necrotrophic fungi *Alternaria brassicicola*, *Botrytis cinerea*, and *Leptosphaeria maculans*, as well as to the oomycete pathogen *Phytophtora brassicae* (Thomma et al., 1999; Bohman et al., 2004; Ferrari et al., 2007; Schlaeppi et al., 2010). In line with previous studies (Zhou et al., 1999; Glawischnig et al., 2004; Nafisi et al., 2007), our data show that *P.*

syringae-induced camalexin accumulation proceeds via the biosynthetic genes *CYP79B2/3*, *CYP71A13* and *PAD3* (Fig. 4; Fig. 5A; Fig. 11A). Further, our mutant analyses indicate that *MYB122* positively regulates *P. syringae*-induced camalexin accumulation (Fig. 4). *MYB122* was recently assigned an accessory role in the regulation of indolic glucosinolate biosynthesis, with *MYB34* and *MYB51* possessing a more dominant regulatory role in this pathway (Frerigmann and Gigolashvili, 2014; Fig. S1). Moreover, MYB122 was shown to positively influence UV light-induced camalexin accumulation (Frerigmann et al., 2015). Thus, several transcription factor genes, including *WRKY33* (Mao et al., 2011), *ANAC042* (Saga et al., 2012), and *MYB122* (this study; Frerigmann et al., 2015) appear to be involved in the regulation of camalexin biosynthesis.

Similar to the biosynthetic mutant *cyp71A13*, both *cyp81f1* and *cyp81f2* display strongly reduced *P. syringae*-induced camalexin accumulation (Fig. 5A). When heterologously expressed in metabolically engineered *Nicotiana benthamiana* plants, Arabidopsis CYP81F1 and CYP81F2 have the biochemical capacity to 1- and 4-hydroxylate I3M, which is required for the formation of the methoxylated I3M derivatives 1- and 4-methoxy-I3M (1- and 4-MeO-I3M), respectively (Pfalz et al., 2011). Whereas *cyp81f2* shows reduced 4-MOI3M levels, corroborating a role for CYP81F2 in I3M methoxylation, *cyp81f1* shows a glucosinolate profile indistinguishable from the wild-type (Pfalz et al., 2011). Notably, the *cyp81F1* and *cyp81F2* mutants share also other metabolic peculiarities with *cyp71A13* (Fig. 5; Fig. 11A). Mutational defects in *CYP71A13, CYP81F1* and *CYP81F2* all result in a marked over-accumulation of I3A and ICA upon *Psm* inoculation (Fig. 5C, D). In addition, the levels of the indole glucosinolate I3M, which decrease in *Psm*-inoculated Col-0 leaves, rise in *cyp81F1*, *cyp81F2*, and *cyp71A13* upon bacterial attack (Fig. S1). And finally, IAN, an I3M hydrolysis product whose levels are virtually not enhanced by *Psm* attack in the wild-type (Kim et al., 2008; Fig. 5B), strongly accumulates in *Psm*-inoculated *cyp71A13, cyp81F1,* and *cyp81F2* (Fig. 5B). It is feasible that in *cyp81F1* and *cyp81F2,* impaired conversion of I3M into methoxylated forms redirects its catabolism towards hydrolytic breakdown and thus hyper-accumulation of substances such as I3A and IAN (Fig. 11A). This could in turn explain ICA over-production, since a biochemical pathway from IAN to ICA exists (Böttcher et al., 2014). By contrast, the strong camalexin-deficient phenotype of *cyp81F1* and *cyp81F2* cannot be readily explained by this supposed redirection of indolic metabolism on the basis of the currently discussed biosynthetic scheme, because over-accumulation of the pathway intermediate IAN should rather favour camalexin production (Fig. 11A). Similarly, over-accumulation of IAN in *cyp71A13* is unexpected, because

recombinant CYP71A13 is able to convert IAOx into IAN (Nafisi et al., 2007), and a defect in the monooxygenase *in planta* is thus expected to result in IAN shortage. Potentially, blockage of the direct IAOx to IAN conversion step in *cyp71A13* redirects the metabolic flow towards indole glucosinolate formation, resulting in increased I3M production and subsequent I3M to IAN hydrolysis (Fig. 11A; Fig. S1). Compared to *cyp71A13, cyp81F1,* and *cyp81F2*, the disturbances of indolic metabolism are more constrained in *pad3*, which is impaired in the final step of camalexin biosynthesis (Schuhegger et al., 2006). Here, the blockage of *Psm*-induced camalexin accumulation results in IAN over-production but does not affect I3A and ICA formation or the degradation of I3M after bacterial inoculation (Fig. 5; Fig. 11A; Fig. S1).

Besides camalexin biosynthesis, indole glucosinolate breakdown leading to I3A accumulation is a major part of indolic metabolism in *P. syringae*-inoculated Col-0 leaves (Fig. 2). I3A accumulation in Arabidopsis is so far documented to occur upon fungal and oomycete but not upon bacterial attack - for instance after leaf inoculation with the non-adapted powdery mildew *Blumeria graminis* f.sp. *hordei*, *Phytophthora brassicae*, *Plectosphaerella cucumerina*, and *Colletotrichum gloeosporioides* (Bednarek et al., 2009; Sanchez-Vallet et al., 2010; Schlaeppi et al., 2010; Hiruma et al., 2013). The determined levels of I3A accumulating in these interactions were between 1 and 10 nmol g^{-1} fresh weight (FW). In *P.syringae*-infected leaves, I3A accumulated to about 50 µg g^{-1} FW at 48 hpi (Fig. 3), which, on a molar basis, corresponds to 340 nmol g^{-1} FW. Therefore, the absolute levels of I3A produced in *P. syringae*-inoculated leaves exceed those previously quantified for fungal inoculations by 1 to 2 orders of magnitude.

Our study reveals a positive regulatory role of the defense hormone SA on I3A production. First, the *P. syringae*-induced levels of I3A are significantly lower in SA-deficient *sid2* and in SA downstream signalling-defective *npr1* than in the wilde-type (Fig. 8). Second, exogenous application of SA is sufficient to trigger I3A elevations with concomitant decreases of the precursor glucosinolate I3M (Fig. 6A). And third, induced I3A accumulation early after *P. syringae*-inoculation is stronger in SA-pretreated than in non-pretreated plants (Fig. 6A). The generation of I3A after fungal attack fully depends on the atypical myrosinase PEN2 (Bednarek et al., 2009; Sanchez-Vallet et al., 2010). Although the production of I3A does not fully correlate with penetration resistance of Arabidopsis against non-adapted powdery mildews if different mutant lines are considered, genetic evidence indicates that indole glucosinolate degradation via PEN2 is a critical determinant of Arabidopsis pre-

invasion resistance to fungal and oomycete pathogens (Bednarek et al., 2009; Sanchez-Vallet et al., 2010; Schlaeppi et al., 2010; Hiruma et al., 2013). I3A accumulation in *P. syringae*-inoculated *pen2* leaves is markedly reduced but not fully abrogated (Fig. 4). This suggests that *P. syringae*-induced I3A is formed via PEN2-dependent and PEN2-independent pathways (Fig. 11A). Microarray data suggest that *PEN2* is not up-regulated by SA after exogenous treatment or *P. syringae* inoculation in Col-0 leaves (Thibaud-Nissen et al., 2006; Wang et al., 2008; Gruner et al., 2013). Taking the above SA regulatory role if I3A production into account, it is possible that another, SA-inducible β-glucosidase contributes to the PEN2-independent pathway of I3A formation from I3M (Fig. 11A).

I3A formation is also markedly impaired in *myb51 and myb51 myb122*. Moreover, the *tmyb* triple knockout line fails to produce I3A in both control and *Psm*-inoculated plants (Fig. 4). Therefore, MYB51 alone and in combination with MYB34 and MYB122, has a major regulatory impact on *P. syringae*-induced I3A biosynthesis (Fig. 11A). This coincides with the regulatory role of *MYB34* and *MYB51* in the biosynthesis of the precursor glucosinolate I3M (Frerigmann and Gigolashvili, 2014; Fig. S1). Even though I3A accumulates to high levels in leaves of wild-type plants during the bacterial interaction, the I3A-depletet *pen2*, *cyp79b2/3*, and *tmyb* lines are not impaired in basal resistance to *Psm* (Fig. 9B), indicating that indole glucosinolate breakdown is not a critical determinant for basal immunity to compatible *P. syringae* bacteria.

The Trp-derived carboxylic acid ICA is an additional indolic compound that accumulates to levels of more than 1 µg g^{-1} FW in *Psm*-inoculated Arabidopsis leaves at 48 hpi, which is quantitatively lower than camalexin or I3A production but in the range of induced SA levels (Figs. 3 and 4). A biochemical pathway involved in the $AgNO_3$-induced formation of ICA and glycosylated ICA-derivatives has been established recently. IAN is thereby converted into the indolic aldehyde ICC by CYP71B6, and ICC is in turn oxidized to ICA by the aldehyde oxidase AAO1 (Böttcher et al., 2014). ICC is also synthesized upon *P. syringae*-inoculation in leaves, albeit to lower amounts than ICA (Fig. 4). ICA, ICC, and hydroxylated and glycosylated derivatives thereof are formed in response to infection by different pathogens or abiotic stress in Arabidopsis roots and leaves (Hagemeier et al., 2001; Bednarek et al., 2005; Böttcher et al., 2009; Gamir et al., 2012). Hydrolysis and chemical analyses of pathogen-treated leaf or root tissue indicate that a portion of the accumulating ICA, along with several benzoic acid and cinnamic acid derivatives, becomes esterified to cell walls upon pathogen-inoculation (Tan et al., 2004; Forcat et al., 2010). From these studies, it

is not clear yet whether free or bound ICA or ICC contribute to plant pathogen resistance. Our study shows that ICA and ICC formation in *P. syringae*-inoculated leaves depends on *cyp79b2/3* and is attenuated in *pen2* and *tmyb* (Fig. 4). This suggests that the hydrolysis of indole glucosinolates contributes to ICA and ICC production upon bacterial inoculation (Fig. 11A). Since the *cyp79b2/3*, *pen2* or *tmyb* mutants do not exhibit defects in basal resistance to *Psm* (Figs. 9, 10), it is unlikely that ICA or ICC represent major resistance determinants against compatible *P. syringae* infection. Our exogenous feeding assays indicate that the resistance-enhancing capacity of ICA in wild-type Col-0 plants is small to non-existent (Fig. S4). However, a modest contribution of ICA to Arabidopsis resistance might exist, if major resistance signalling components such as PAD4 or NPR1 are dysfunctional (Fig. S4C).

Systemic indole accumulation and its functional relevance for SAR

Notably, our results show that indolic metabolism is activated systemically when plants experience a locally restricted leaf inoculation with *P. syringae*. The metabolic response in leaves distant from the site of bacterial attack is quantitatively milder than the local response and specifically involves the accumulation of I3A, ICA, and ICC (Fig. 2). Thus, the three indoles share the relatively rare feature to systemically accumulate in the plant upon a localized bacterial inoculation with the SAR regulatory metabolites Pip and SA (Návarová et al., 2012; Zeier, 2013). Among them, I3A is produced to highest levels in the distal leaf tissue, reaching values of about 10 µg g^{-1} FW upon inoculation (Figs. 2 and 7). The absolute I3A levels after SAR activation are therefore in a similar range than the levels of Pip and higher than those of SA (Návarová et al., 2012).

The regulatory principles of *P. syringae*-induced I3A, ICA, and ICC formation differ in locally inoculated and in systemic tissue. First, systemic but not local indole accumulation requires the Pip and SA biosynthetic genes *ALD1* and *ICS1* (alias *SID2*) as well as intact *FMO1* and *NPR1* (Fig. 8). Therefore, functional SAR signaling, which involves Pip and SA accumulation, is required for the systemic but not for the local accumulation of I3A, ICA, and ICC. Second, the systemic production of I3A, ICA, and ICC is totally absent in the *pen2* and *tmyb* mutant lines, whereas their local accumulation is not fully compromised (Figs. 4 and 7). This indicates that MYB34/51/122-regulated biosynthesis of indole glucosinolates and their PEN2-mediated breakdown are obligatory for the *P. syringae*-induced accumulation of I3A, ICA, and ICC in systemic leaf tissue (Fig. 7, Fig. S1; Bednarek et al., 2009; Frerigmann and Gigolashvili, 2014). The ability of the *ald1*, *fmo1*, *sid2*, and *npr1* lines of local indole

production and their failure of systemic indole elevation also indicate that I3A, ICA, and ICC are synthesized de novo in distal tissue in context with SAR establishment rather than by long-distance transport from locally infected to uninfected, systemic leaves.

After recognizing the systemic activation of indolic metabolism in *P. syringae*-inoculated Arabidopsis plants, a major aim of the current study was to test whether the systemically accumulating indoles would be functionally relevant for SAR. A previous finding that exogenous 3-acetonyl-3-hydroxyoxindole, an oxidized indole derivative isolated from extracts of the Assam Indigo plant *Strobilanthes cusia*, activates the SA pathway and a SAR-like response in tobacco further pointed to this possibility (Li et al., 2008). Since *tmyb*, *pen2*, and *cyp79b2/3* failed to systemically elevate I3A, ICA, and ICC, and *myb34*, *myb51*, and *myb51 myb122* had a significantly weaker systemic response than the wild-type (Fig. 7; Fig. S2B), we were directly able to test this hypothesis. Bacterial growth assays with *P. syringae* as the inducing and the challenging pathogen demonstrated, however, that the systemic accumulation of the indolics is not a decisive event for SAR establishment. First, soil-grown *tmyb* triple and *myb* single and double mutants were able to systemically enhance resistance to 2° bacterial challenge when inoculated in 1° leaves with *Psm* (Fig. 10). Along with this, an inducing leaf inoculation also resulted in significantly elevated levels of SA in distal leaves of *tmyb* and *myb* single and double mutant plants (Fig. S5). Second, the *cyp79b2/3* and *pen2* mutants were able to induce a wild-type-like SAR response when grown in hydroponic culture, and this was again associated with increase of SA in distal leaves upon *Psm* inoculation of 1° leaves (Fig. 9A, C). The activation of SAR towards *P. syringae* and the associated activation of the SA pathway are therefore independent of the systemic accumulation of indolics.

Our data thus indicate that increased systemic de novo production of I3A, ICA, and ICC is a consequence rather than the cause of SAR activation, for which Pip and SA are the essential, signaling active metabolites (Nawrath and Métraux, 1999; Návarová et al., 2012; Fig. 8A). However, although the elevated levels of indolics during SAR do not contribute to resistance induction towards the bacterial hemibiotroph *P. syringae*, they might well increase defense readiness against other pathogen types, because indole glucosinate breakdown products such as I3A are discussed as antifungal compounds providing direct protection against non-adapted and adapted fungal or oomycete pathogens (Bednarek et al., 2009; Sanchez-Vallet et al., 2010; Schlaeppi et al., 2010; Consonni et al., 2010; Bednarek, 2012; Hiruma et al., 2013). The well-established SAR assay system that uses Arabidopsis and

P syringae as the inducing and the challenging pathogen is predominantly employed in the current SAR research to study the mechanisms of SAR activation (Shah and Zeier, 2013). However, this system does not yield information about the broadness of resistance activation in SAR. To investigate the broad-spectrum character of SAR (Sticher et al., 1997) and the contributions of individual defense pathways in the protection against a particular pathogen, assays with different types of challenging pathogens should be developed in the future and combined with mutant analyses.

Cultivation-dependent pre-induced immunity in *cyp79b2/3* and *pen2* dampens *P. syringae*-triggered SAR

To varying degrees between individual experiments, soil-grown *cyp79b2/3* and *pen2* plants exhibited enhanced basal resistance and contained elevated SA levels, tendencies that were absent or only marginally observed in hydroponically cultivated plants (Fig. 9B, C). This suggests that soil cultivation-dependent factors pre-activate inducible immune responses such as the SA pathway in *cyp79b2/3* and *pen2* but not in the wild-type (Fig. 11B). Since CYP79B2/3 and PEN2 are essential components of pre-invasion immunity that underlie non-host resistance (Lipka et al., 2005; Bednarek et al., 2009; Schlaeppi et al., 2010), defects in early immune layers seem to entail the activation of later layers, i.e. inducible defense responses, under certain growth conditions. Consistently, constitutively activated SA defences were also observed for mutants defective in *PEN1* and *PEN3,* encoding a syntaxin and an ATP binding cassette transporter, respectively, that constitute other critical elements of Arabidopsis pre-penetration resistance to fungal ingress (Collins et al., 2003; Stein et al., 2006; Zhang et al., 2007). A speculative scenario is that soil-inhabiting microbes failing to overcome pre-invasion immune layers in the wild-type can pass these early obstacles in *cyp79b2/3* and *pen2*, and as a consequence, continuously elicit inducible, post-invasion responses in the course of plant growth. Plants thereby lose their naïve character and increase resistance to adapted pathogens (Fig. 11B). This "pre-formed" immunity then apparently alleviates a further strong resistance enhancement upon inoculation with a SAR-inducing pathogen, which is observed in the naïve wild-type (Fig. 11B). The SAR-positive phenotype of hydroponically-grown, not pre-induced *cyp79b2/3* and *pen2* plants indicate their intrinsic ability to induce SAR. Interestingly, loss of *PEN1*, *PEN2*, *PEN3*, and *CYP79B2/3* attenuates the hypersensitive cell death response triggered by *P. syringae* effectors (Johansson et al.,

2014), indicating that inducible immune responses other than SAR are affected if early plant immune layers are dysfunctional.

METHODS

Plant material and cultivation

For soil cultivation, *Arabidopsis thaliana* plants were grown in individual pots containing a mixture of soil (Klasmann-Deilmann, Substrat BP3) vermiculite, and sand (8:1:1). Plants cultivated in hydroponic culture (Araponics system) (Tocquin et al., 2003) were grown in a medium containing the following nutrients: 1.50 mM $Ca(NO_3)_2$, 1.25 mM KNO_3, 0.75 mM $MgSO_4$, 0.50 mM KH_2PO_4, 0.1 mM Na_2O_3Si, 72 µM Fe-EDTA, 50 µM KCl, 50 µM H_3BO_3, 10 µM $MnSO_4$, 2 µM $ZnSO_4$, 1.5 µM $CuSO_4$, 0.075 µM $(NH_4)_6Mo_7O_{24}$ and the final pH was set up to 6.0 (Gibeaut et al., 1997). The seed-holders were filled with 0.6 % agar. Soil- and hydroponically-cultivated plants were grown inside a controlled environmental chamber with a 10 h day (9 $_{AM}$ to 7 $_{PM}$; photon flux density 100 µmol m^{-2} s^{-1}) / 14 h night cycle and relative humidity of 60%. Temperatures during the day and night period were 21 and 18 °C, respectively.

The *cyp81f1* mutant corresponds to the SALK T-DNA insertion lines SALK_031939 (Pfalz et al., 2011), and the *myb122* mutant corresponds to SALK_022993. Homozygous T-DNA insertion lines were identified by PCR according to Alonso et al. (2003) with the following gene-specific primers (sequences 5' to 3'): *cyp81f1* - CATACAACCACACAACCGTTG (LP) and CCTCCCAAATCTCTGGATCTC (RP); *myb122* - AGCAGAAGGGTTGAAGAAAGG (LP) and GGGGAGATTCGAAGAGGTATG (RP). Other lines used in this study are *cyp79b2 cyp79b3* (*cyp79b2/3*; Zhao et al., 2002), *pen2-2* (*pen2*; Lipka et al., 2005), *cyp81f2-1* (*cyp81f2;* Bednarek et al., 2009), *cyp71a13-1* (*cyp71a13*; Nafisi et al., 2007), *pad3-1* (*pad3*; Glazebrook and Ausubel, 1994), *myb34*, *myb51*, *myb34 myb51 myb122* (*tmyb*; Frerigmann and Gigolashvili, 2014), *myb51 myb122* (Frerigmann et al., 2015), *ald1* (Návarová et al., 2012), *fmo1* (Mishina and Zeier, 2006), *sid2* (*sid2-1*; Nawrath and Métraux, 1999), *pad4-1* (*pad4*; Jirage et., 1999), *npr1-2* (*npr1*; NASC ID N3801), *coi1-35* (*coi1*; Staswick and Tiryaki, 2004). All mutant lines are in the Col-0 background.

Cultivation of Bacteria

Pseudomonas syringae pv. *maculicola* strain ES4326 (*Psm*), and *Psm* carrying the *avrRpm1* avirulence gene (*Psm avrRpm1*), were grown in King´s B medium containing the appropriate antibiotics (Zeier et al., 2004). Overnight log phase cultures were washed three times with 10 mM $MgCl_2$ and diluted to different optical densities at 600 nm (OD_{600}) for leaf inoculation. The bacterial solutions were infiltrated from the abaxial side into the leaves.

Assessment of basal resistance and SAR

For measurement of basal resistance, three leaves per plant were infiltrated with a suspension of *Psm* at OD_{600} 0.001 between 10 and 12 $_{AM}$. 2.5 d after the treatment, the amount of bacteria in the inoculated leaves was quantified as described (Návarová et al., 2012). To induce SAR, three lower (1°) leaves per plant were infiltrated with a suspension of *Psm* at OD_{600} 0.005. Control plants were infiltrated with a 10 mM $MgCl_2$ solution. For SAR growth assay, three upper leaves (2°) of all pretreated plants were infiltrated with a suspension of *Psm* at OD_{600} 0.001 two days after the first treatment. The growth of bacteria in these leaves was quantified as described (Návarová et al., 2012).

For metabolite profiling, three 1° leaves per plant were infiltrated with a suspension of *Psm* at OD_{600} 0.005. Control plants were infiltrated with a 10 mM $MgCl_2$ solution. Regularly two days after this treatment, samples from 1° inoculated leaves and 2° untreated leaves were harvested, fresh weights were determined, and samples were used for metabolite analyses (except for time-course analysis depicted in Fig. 3).

Determination of indolic metabolites and SA via GC/MS

Determination of metabolites listed in Table 1 and SA was performed as outlined previously (Návarová et al., 2012), using vapor-phase extraction and subsequent analysis by gas chromatography coupled with mass spectrometric detection (GC/MS). For comparative metabolite profiling, individual ion chromatograms (m/z between 50 and 300) resulting from sample extracts of Col-0 and *cyp79b2/3* leaves were screened. Substance peaks were identified by comparison of mass spectra and retention times with those of authentic standards, or by matching of recorded mass spectra with spectra of the NIST library. The identification mode is indicated in Table 1. For quantification, peaks emanating from selected ion chromatograms [*m/z*] were integrated. The *m/z* values for quantification are depicted in Table 1. The resulting peak areas were expressed relative to the peak area of the internal

standard indole-3-propionic acid (IPA) [*m/z* 130], and expressed relative to the leaf sample fresh weight. Peak areas for SA [*m/z* 120] were expressed relative to those of the internal standard D_4-SA [*m/z* 124].

Determination of Trp was performed as described in Návarová et al. (2012) using the EZ:faast free amino acid kit for GC/MS (Phenomenex).

Metabolite determination via HPLC

Determination of I3A and I3M was performed by high performance liquid chromatography (HPLC) coupled with fluorescence detection. Homogenized leaf material was mixed with 520 µl DMSO (containing IPA – 1 ng/µl), the mixture was shaken thoroughly for 5 minutes and centrifuged for 20 min at 13200 rpm. 450 µl of the supernatant was transferred into a new reaction tube and centrifuged again for 5 min at 13200 rpm. 400 µl of the supernatant was transferred into a new reaction tube and a 5 µl aliquot was subjected to HPLC analysis. The injected sample mixture was separated on a high-performance liquid chromatograph (1260 Infinity; Agilent Technologies) equipped with a C18 column (Zorbax SB-C18, 2.1x100 mm, 1.8 µm; Agilent Technologies) with water (0.01% formic acid) as solvent A and 98% acetonitrile (2% H_2O; 0.01% formic acid) as solvent B at a flow rate of 0.250 ml/min and at 27 °C (gradient of solvent B: 3% for 4 min, to 9% in 5 min, to 11% in 6 min, to 28% in 15 min, to 60% in 10 min, to 100% in 10 min, 100% for 5 min, to 0% in 2 min, 0% for 4 min, to 3% in 1 min, 3% for 5 min). Peaks were detected with a fluorescence detector (1260 Infinity Fluorescence Detector; Agilent Technologies) by an excitation of 275 nm and an emission of 350 nm. For quantification, the corresponding peaks were integrated and areas were expressed relative to the peak area of the internal standard IPA.

Exogenous application of Pip, SA, and ICA

For metabolite feeding via the root system, plants were supplemented with aqueous solutions of 10 ml of 1mM $_{D,L}$-Pip or ICA via the soil one day prior to bacterial inoculation (Návarová et al., 2012). ICA (S220027; Sigma Aldrich) was diluted in an equimolar solution of NaOH, and the pH was set to 7.0. Control plants were supplemented with 10 ml of water.

For exogenous leaf treatments, solutions of 0.5 mM SA or ICA were infiltrated into three leaves of five-week-old plants. Water was infiltrated as a control treatment. To determine plant resistance to *Psm*, bacterial suspension (OD_{600} 0.001) were infiltrated into the

same leaves 4 h later, and bacterial growth was assessed as described above. For metabolite analyses, SA- or water-pretreated leaves received one of the following secondary treatments 4 h after the pre-treatment: *Psm*-infiltration with a suspension of OD_{600} 0.005, mock-infiltration with 10 mM $MgCl_2$, or no treatment at all. Leaf samples for metabolite analyses were harvested 10h, 24h, and 48h after the second treatment.

Statistical analyses and reproducibility of experiments

Statistical analyses of pairwise compared samples were performed using Student's *t* test. The relative tendencies of the depicted results were confirmed in at least two biologically independent experiments.

Accession numbers

Sequence Data from the major genes described in this article can be found in the Arabidopsis Genome Initiative or GenBank/EMPL databases under the following accession numbers: *CYP79B2* (At4g39950), *CYP79B3* (At2g22330), *PEN2* (At2g44490), *CYP81F1* (At4g37430), *CYP81F2* (At5g57220), *CYP71A13* (At2g30770), *PAD3* (At3g26830), *PAD4* (At3g52430), *MYB34* (At5g60890), *MYB51* (At1g18570), *MYB122* (At1g74080), *ALD1* (At2g13810), *FMO1* (At1g19250), *ICS1* (At1g74710), *COI1* (At2g39940), and *NPR1* (At1g64280).

SUPPLEMENTAL INFORMATION

Supplemental Information is available at *Molecular Plant Online*.

FUNDING

This work was supported by the German Research Foundation (DFG Cluster of Excellence on Plant Sciences and DFG Graduate program IRTG 1525), and the Swiss National Science Foundation (SNF grant No. 3100A-125374).

AUTHOR CONTRIBUTIONS

E.S., P.B., S.H., K.S., F.B., and J.Z. performed and evaluated the experiments. A.V.-M. provided expertise in LC analyses, and F.M. provided supervision and feedback. E.S. assisted J.Z. in manuscript preparation and writing. J.Z. designed the research, wrote the manuscript, and secured funding.

ACKNOWLEDGMENTS

We thank Tamara Gigolashvili and Henning Frerigmann for providing *myb34*, *myb51*, *myb51 myb122*, and *tmyb* seeds, Pavel Bednarek for allocating *cyp81f2-1* seeds and authentic I3A standard, Volker Lipka for providing *pen2-2* seeds, and Reinhard Neier for support on LC-based metabolite analyses.

REFERENCES

Alonso, J.M., Stepanova, A.N., Leisse, T.J., Kim, C.J., Chen, H.M., Shinn, P., Stevenson, D.K., Zimmerman, J., Barajas, P., Cheuk, R., et al. (2003). Genome-wide insertional mutagenesis of *Arabidopsis thaliana*. Science. **301,** 653-657.

Attaran, E., Rostás, M., and Zeier, J. (2008). *Pseudomonas syringae* elicits emission of the terpenoid (E,E)-4,8,12-trimethyl-1,3,7,11-tridecatetraene in *Arabidopsis* leaves via jasmonate signaling and expression of the terpene synthase TPS4. Mol Plant Microbe Interact. 2008 Nov;21(11):1482-97. Mol. Plant Microbe Interact. **21**, 1482-1497.

Attaran, E., Zeier, T.E., Griebel, T., and Zeier, J. (2009). Methyl salicylate production and jasmonate signaling are not essential for systemic acquired resistance in Arabidopsis. Plant Cell. **21**, 954-971.

Bednarek, P. (2012). Chemical warfare or modulators of defence responses - the function of secondary metabolites in plant immunity. Curr. Opin. Plant. Biol. **15**, 407-414.

Bednarek, P., and Osbourn, A. (2009). Plant-microbe interactions: chemical diversity in plant defense. Science. **324**, 746-748.

Bednarek, P., Piślewska-Bednarek, M., Svatoš, A., Schneider, B., Doubský, J., Mansurova, M., Humphry, M., Consonni, C., Panstruga, R., Sanchez-Vallet, et al. (2009). A glucosinolate metabolism pathway in living plant cells mediates broad-spectrum antifungal defense. Science. **323**, 101-106.

Bednarek, P., Piślewska-Bednarek, M., Ver Loren van Themaat, E., Maddula, R.K., Svatoš, A., and Schulze-Lefert, P. (2011). Conservation and clade-specific diversification of pathogen-inducible tryptophan and indole glucosinolate metabolism in *Arabidopsis thaliana* relatives. New Phytol. **192**,713-726.

Bednarek, P., Schneider, B., Svatos, A., Oldham, N.J., and Hahlbrock, K. (2005). Structural complexity, differential response to infection, and tissue specificity of indolic and phenylpropanoid secondary metabolism in Arabidopsis roots. Plant Physiol. **138**, 1058-1070.

Bender, J., and Celenza, J.L. (2009). Indolic glucosinolates at the crossroads of tryptophan metabolism. Phytochem. Rev. **8**, 25-37.

Bernsdorff, F., Döring A.-C., Gruner, K., Schuck, S., Bräutigam, A., and Zeier, J. (2016). Pipecolic acid orchestrates plant systemic acquired resistance and defense priming

via salicylic acid-dependent and -independent pathways. Plant Cell. doi:10.1105/tpc.15.00496.

Bisgrove, S.R., Simonich, M.T., Smith, N.M., Sattler, A., and Innes, R.W. (1994). A disease resistance gene in Arabidopsis with specificity for two different pathogen avirulence genes. Plant Cell. **6**, 927-933.

Bohman, S., Staal, J., Thomma, B.P., Wang, M., and Dixelius, C. (2004). Characterisation of an Arabidopsis-*Leptosphaeria maculans* pathosystem: resistance partially requires camalexin biosynthesis and is independent of salicylic acid, ethylene and jasmonic acid signaling. Plant J. **37**, 9-20.

Böttcher, C., Chapman, A., Fellermeier, F., Choudhary, M., Scheel, D., and Glawischnig, E. (2014). The biosynthetic pathway of indole-3carbaldehyde and indole-3-carboxylic acid derivatives in *Arabidopsis thaliana*. Plant Physiol. **165**, 841-853.

Böttcher, C., Westphal, L., Schmotz, C., Prade, E., Scheel, D., and Glawischnig, E. (2009). The Multifunctional Enzyme CYP71B15 (PHYTOALEXIN DEFICIENT3) Converts Cysteine-Indole-3-Acetonitrile to Camalexin in the Indole-3-Acetonitrile Metabolic Network *of Arabidopsis thaliana*. Plant Cell. **21**, 1830-1845.

Brown, P.D., Tokuhisa, J.G., Reichelt, M., and Gershenzon J. (2003). Variation of glucosinolate accumulation among different organs and developmental stages of *Arabidopsis thaliana*. Phytochemistry. **62**, 471-481.

Collins, N.C., Thordal-Christensen, H., Lipka, V., Bau, S., Kombrink, E., Qiu, J.L., Hückelhoven, R., Stein, M., Freialdenhoven, A., Somerville, S.C., and Schulze-Lefert, P. (2003). SNARE-protein-mediated disease resistance at the plant cell wall. Nature. **425**, 973-977.

Consonni, C., Bednarek, P., Humphry, M., Francocci, F., Ferrari, S., Harzen, A., Ver Loren van Themaat, E., and Panstruga, R. (2010). Tryptophan-derived metabolites are required for antifungal defense in the Arabidopsis *mlo2* mutant. Plant Physiol. **152**, 1544-1561.

Ferrari, S., Galletti, R., Denoux, C., De Lorenzo, G., Ausubel, F.M., and Dewdney J. (2007). Resistance to *Botrytis cinerea* induced in Arabidopsis by elicitors is independent of salicylic acid, ethylene, or jasmonate signaling but requires PHYTOALEXIN DEFICIENT3. Plant Physiol. **144**, 367-379.

Feys, B.J., Moisan, L.J., Newman, M.A., and Parker, J.E. (2001). Direct interaction between the *Arabidopsis* disease resistance signaling proteins, EDS1 and PAD4. EMBO J. **20**, 5400-5411.

Forcat, S., Bennett, M., Grant, M., and Mansfield, J.W. (2010). Rapid linkage of indole carboxylic acid to the plant cell wall identified as a component of basal defence in Arabidopsis against *hrp* mutant bacteria. Phytochemistry. **71**, 870-876.

Frerigmann, H., and Gigolashvili, T. (2014). MYB34, MYB51, and MYB122 Distinctly Regulate Indolic Glucosinolate Biosynthesis in *Arabidopsis thaliana*. Mol. Plant. **7**, 814-828.

Frerigmann, H., Glawischnig, E., and Gigolashvili, T. (2015). The role of MYB34, MYB51, and MYB122 in the regulation of camalexin biosynthesis in *Arabidopsis thaliana*. Front. Plant Sci. **6**, 654. doi: 10.3389/fpls/2015.00654.**Fu, Z.Q., and Dong, X.** (2013). Systemic acquired resistance: turning local infection into global defense. Annu. Rev. Plant Biol. **64**, 839-863.

Gamir, J., Pastor, V., Cerezo, M., and Flors, V. (2012). Identification of indole-3-carboxylic acid as mediator of priming against *Plectosphaerella cucumerina*. Plant Physiol. Biochem. **61**, 169-179.

Geu-Flores, F., Møldrup, M.E., Böttcher, C., Olsen, C.E., Scheel, D., and Halkier, B.A. (2011). Cytosolic γ-glutamyl peptidases process glutathione conjugates in the biosynthesis of glucosinolates and camalexin in *Arabidopsis*. Plant Cell. **23**, 2456-2469.

Gibeaut, D.M., Hulett, J., Cramer, G.R., and Seemann, J.R. (1997). Maximal Biomass of *Arabidopsis thaliana* Using a Simple, Low-Maintenance Hydroponic Method and Favorable Environmental Conditions. Plant Physiol. **115**, 317-319.

Gigolashvili, T., Berger, B. and Flügge, U.I. (2009). Specific and coordinated control of indolic and aliphaticglucosinolate biosynthesis by R2R3-MYB transcription factors in *Arabidopsis thaliana*. Phytochemistry. Rev. **8**, 3-13.

Glawischnig, E. (2007). Camalexin. Phytochemistry. **68**, 401-406.

Glawischnig, E., Hansen, B.G., Olsen, C.E., and Halkier, B.A. (2004). Camalexin is synthesized from indole-3-acetaldoxime, a key branching point between primary and secondary metabolism in *Arabidopsis*. Proc. Natl Acad. Sci. USA. **101**, 8245-8250.

Glazebrook, J., and Ausubel, F.M. (1994). Isolation of phytoalexin-deficient mutants of *Arabidopsis thaliana* and characterization of their interactions with bacterial pathogens. Proc. Natl Acad. Sci. USA. **91**, 8955–8959.

Griebel, T., and Zeier, J. (2010). A role for β-sitosterol to stigmasterol conversion in plant-pathogen interactions. Plant J. **63**, 254-268.

Gruner, K., Griebel, T., Návarová H., Attaran, E., and Zeier J. (2013). Reprogramming of plants during systemic acquired resistance. Front in Plant Sci. **4**, 252.

Hagemeier, J., Schneider, B., Oldham, N.J., and Hahlbrock K. (2001). Accumulation of soluble and wall-bound indolic metabolites in *Arabidopsis thaliana* leaves infected with virulent or avirulent *Pseudomonas syringae* pathovar tomato strains. Proc. Natl Acad. Sci. USA. **98**, 753-758.

Hagemeier, J., Schneider, B., Oldham, N.J., and Hahlbrock, K. (2001). Accumulation of soluble and wall-bound indolic metabolites in *Arabidopsis thaliana* leaves infected with virulent or avirulent *Pseudomonas syringae* pathovar tomato strains. Proc. Natl Acad. Sci. USA. **98**, 753-758.

Hiruma, K., Fukunaga, S., Bednarek, P., Pislewska-Bednarek, M., Watanabe, S., Narusaka, Y., Shirasu, K., and Takano, Y. (2013). Glutathione and tryptophan metabolism are required for *Arabidopsis* immunity during the hypersensitive response to hemibiotrophs. Proc. Natl Acad. Sci. USA. **110**, 9589-9594.

Iven, T., König, S., Singh, S., Braus-Stromeyer, S.A., Bischoff, M., Tietze, L.F., Braus, G.H., Lipka, V., Feussner, I., and Dröge-Laser, W. (2012). Transcriptional activation and production of tryptophan-derived secondary metabolites in *Arabidopsis* roots contributes to the defense against the fungal vascular pathogen *Verticillium longisporum*. Mol. Plant. **5**, 1389-13402.

Jirage, D., Tootle, T.L., Reuber, T.L., Frost, L.N., Feys, B.J., Parker, J.E., Ausubel, F.M., and Glazebrook, J. (1999). *Arabidopsis thaliana* PAD4 encodes a lipase-like gene that is important for salicylic acid signaling. Proc. Natl Acad. Sci. USA. **96**, 13583–13588.

Johansson, O.N., Fantozzi, E., Fahlberg, P., Nilsson, A.K., Buhot, N., Tör, M., and Andersson, M.X. (2014). Role of the penetration-resistance genes *PEN1*, *PEN2* and

PEN3 in the hypersensitive response and race-specific resistance in *Arabidopsis thaliana*. Plant J. **79**, 466-476.

Jones, J.D.G. and Dangl, J.L. (2006). The plant immune system. Nature. **444**, 323-329.

Kim, J.H., Lee, B.W., Schroeder, F.C., and Jander G. (2008). Identification of indole glucosinolate breakdown products with antifeedant effects on *Myzus persicae* (green peach aphid). Plant J. **54**, 1015-1026.

Kliebenstein, D.J., Rowe, H.C., and Denby, K.J. (2005). Secondary metabolites influence Arabidopsis/*Botrytis* interactions: variation in host production and pathogen sensitivity. Plant J. **44,** 25–36.

Li, Y., Zhang, Z., Jia, Y., Shen, Y., He, H., Fang, R., Chen, X., and Hao, X. (2008). 3-Acetonyl-3-hydroxyoxindole: a new inducer of systemic acquired resistance in plants. Plant Biotechnol J. **6**, 301-308.

Lipka, V., Dittgen, J., Bednarek, P., Bhat, R., Wiermer, M., Stein, M., Landtag, J., Brandt, W., Rosahl, S., Scheel, D., et al. (2005). Pre- and postinvasion defenses both contribute to nonhost resistance in *Arabidopsis*. Science. **310**, 1180-1183.

Malitsky, S., Blum, E., Less, H., Venger, I., Elbaz, M., Morin, S., Eshed, Y., and Aharoni, A. (2008). The transcript and metabolite networks affected by the two clades of Arabidopsis glucosinolate biosynthesis regulators. Plant Physiol. **148**, 2021-2049

Mao, G., Meng, X., Liu, Y., Zheng, Z., Chen, Z., and Zhang, S. (2011). Phosphorylation of a WRKY transcription factor by two pathogen-responsive MAPKs drives phytoalexin biosynthesis in *Arabidopsis*. Plant Cell. **23**, 1639-1653.

Mishina, T.E., and Zeier, J. (2006). The Arabidopsis flavin-dependent monooxygenase FMO1 is an essential component of biologically induced systemic acquired resistance. Plant Physiol. **141**, 1666-1675.

Mishina, T.E., and Zeier, J. (2007). Pathogen-associated molecular pattern recognition rather than development of tissue necrosis contributes to bacterial induction of systemic acquired resistance in Arabidopsis. Plant J. **50**, 500-513.

Nafisi, M., Goregaoker, S., Botanga, C.J., Glawischnig, E., Olsen, C.E., Halkier, B.A., and Glazebrook, J. (2007). *Arabidopsis* cytochrome P450 monooxygenase 71A13 catalyzes the conversion of indole-3-acetaldoxime in camalexin synthesis. Plant Cell. **19**, 2039-2052.

Návarová, H., Bernsdorff, F., Döring, A.C., and Zeier J. (2012). Pipecolic acid, an endogenous mediator of defense amplification and priming, is a critical regulator of inducible plant immunity. Plant Cell. **24**, 5123-5141.

Nawrath, C., and Métraux, J.P. (1999) Salicylic acid induction-deficient mutants of Arabidopsis express *PR-2* and *PR-5* and accumulate high levels of camalexin after pathogen inoculation. Plant Cell. **11**, 1393–1404.

Papadopoulou, K., Melton, R.E., Leggett, M., Daniels, M.J., and Osbourn, A.E. (1999). Compromised disease resistance in saponin-deficient plants. Proc. Natl Acad. Sci. USA. **96**, 12923-12928.

Pfalz. M., Mikkelsen, M.D., Bednarek, P., Olsen, C.E., Halkier, B.A., and Kroymann J. (2011). Metabolic engineering in *Nicotiana benthamiana* reveals key enzyme functions in *Arabidopsis* indole glucosinolate modification. Plant Cell. **23**, 716-729.

Saga, H., Ogawa, T., Kai, K., Suzuki, H., Ogata, Y., Sakurai, N., Shibata, D., and Ohta, D. (2012). Identification and Characterization of *ANAC042*, a TranscriptionFactor Family Gene Involved in the Regulation of Camalexin Biosynthesis in *Arabidopsis*. Mol. Plant. Microbe Interact. **25**, 684-696.

Sanchez-Vallet, A., Ramos, B., Bednarek, P., López, G., Piślewska-Bednarek, M., Schulze-Lefert, P., and Molina, A. (2010). Tryptophan-derived secondary metabolites in *Arabidopsis thaliana* confer non-host resistance to necrotrophic *Plectosphaerella cucumerina* fungi. Plant J. **63**, 115-127.

Schlaeppi, K., Abou-Mansour, E., Buchala, A., and Mauch, F. (2010). Disease resistance of Arabidopsis to *Phytophtora brassicae* is established by sequential action of indole glucosinolates and camalexin. Plant J. **62**, 840-851.

Schuhegger, R., Nafisi, M., Mansourova, M., Petersen, B.L., Olsen, C.E., Svatos, A., Halkier, B.A., and Glawischnig, E. (2006). CYP71B15 (PAD3) catalyzes the final step in camalexin biosynthesis. Plant Physiol. **141**, 1248-1254.

Schuhegger, R., Rauhut, T., and Glawischnig, E. (2007). Regulatory variability of camalexin biosynthesis. J. Plant Physiol. **164**, 636-644.

Shah, J., and Zeier, J. (2013). Long-distance communication and signal amplification in systemic acquired resistance. Front. Plant. Sci. **4**, 30.

Singh, P., Yekondi, S., Chen, P.W., Tsai, C.H., Yu, C.W., Wu, K., and Zimmerli, L. (2014). Environmental history modulates Arabidopsis pattern-triggered immunity in a HISTONE ACETYLTRANSFERASE1-dependent manner. Plant Cell. **26**, 2676-2688.

Snyder, B.A., and Nicholson, R.L. (1990). Synthesis of phytoalexins in sorghum as a site-specific response to fungal ingress. Science. **248**, 1637-1639.

Sønderby, I.E, Geu-Flores, F., and Halkier, B.A. (2010). Biosynthesis of glucosinolates--gene discovery and beyond. Trends Plant Sci. **15**, 283-290.

Song, J.T., Lu, H., McDowell, J.M., and Greenberg, J.T. (2004). A key role for ALD1 in activation of local and systemic defenses in *Arabidopsis*. Plant J. **40**, 200-212.

Spoel, S.H., and Dong, X. (2012). How do plants achieve immunity? Defence without specialized immune cells. Nat. Rev. Immunol. **12**, 89-100.

Staswick, P.E., and Tiryaki, I. (2004). The oxylipin signal jasmonic acid is activated by an enzyme that conjugates it to isoleucine in Arabidopsis. Plant Cell. **16**, 2117-2127.

Stein, M., Dittgen, J., Sánchez-Rodríguez, C., Hou, B.H., Molina, A., Schulze-Lefert, P., Lipka, V., and Somerville, S. (2006). *Arabidopsis* PEN3/PDR8, an ATP binding cassette transporter, contributes to nonhost resistance to inappropriate pathogens that enter by direct penetration. Plant Cell. **18**, 731-746.

Sticher, L., Mauch-Mani, B., and Métraux, J.P. (1997). Systemic acquired resistance. Annu. Rev. Phytopathol. **35**, 235-270.

Su, T., Xu, J., Li, Y., Lei, L., Zhao, L., Yang, H., Feng, J., Liu, G., and Ren, D. (2011). Glutathione-indole-3-acetonitrile is required for camalexin biosynthesis in *Arabidopsis thaliana*. Plant Cell. **23**, 364-380.

Tan, J., Bednarek, P., Liu, J., Schneider, B., Svatos, A., and Hahlbrock, K. (2004). Universally occurring phenylpropanoid and species-specific indolic metabolites in infected and uninfected *Arabidopsis thaliana* roots and leaves. Phytochemistry. **65**, 691-699.

Thibaud-Nissen, F., Wu, H., Richmond, T., Redman, J. C., Johnson, C., Green, R., Arias, J., and Town, C.D. (2006). Development of Arabidopsis whole-genome microarrays and their application to the discovery of binding sites for the TGA2 transcription factor in salicylic acid-treated plants. Plant J. **47,** 152-162.

Thomma, B.P., Nelissen, I., Eggermont, K., and Broekaert W.F. (1999). Deficiency in phytoalexin production causes enhanced susceptibility of *Arabidopsis thaliana* to the fungus *Alternaria brassicicola*. Plant J. **19**, 163-171.

Thordal-Christensen, H. (2003). Fresh insights into processes of nonhost resistance. Curr. Opin. Plant Biol. **6,** 351-357.

Tocquin, P., Corbesier, L., Havelange, A., Pieltain, A., Kurtem, E., Bernier, G., and Périlleux, C. (2003). A novel high efficiency, low maintenance, hydroponic system for synchronous growth and flowering of *Arabidopsis thaliana*. BMC Plant Biol. **3**, 2. doi: 10.1186/1471-2229-3-2.

Tsuji, J., Jackson, E.P., Douglas A. Gage, D.A., Hammerschmidt, R., and Somerville S.C. (1992). Phytoalexin accumulation in *Arabidopsis thaliana* during the hypersensitive reaction to *Pseudomonas syringae* pv *syringae*. Plant Physiol. **98**, 1304–1309.

Vlot, A.C., Dempsey, D.A., and Klessig, D.F. (2009). Salicylic Acid, a multifaceted hormone to combat disease. Annu. Rev. Phytopathol. **47**, 177-206.

Vogel-Adghough, D., Stahl, E., Návarová, H., and Zeier J. (2013). Pipecolic acid enhances resistance to bacterial infection and primes salicylic acid and nicotine accumulation in tobacco. Plant Signal. Behav. **8**, 11.

Wang, L., Mitra, R.M., Hasselmann, K.D., Sato, M., Lenarz-Wyatt, L., Cohen, J.D., Katagiri, F., and Glazebrook, J. (2008). The genetic network controlling the Arabidopsis transcriptional response to *Pseudomonas syringae* pv. *maculicola*: roles of major regulators and the phytotoxin coronatine. Mol. Plant-Microbe Interact. **21**,1408–1420.

Wildermuth, M.C., Dewdney, J., Wu, G., and Ausubel, F.M. (2001). Isochorismate synthase is required to synthesize salicylic acid for plant defence. Nature. **414**, 562-565.

Wu, Y., Zhang, D., Chu, J. Y., Boyle, P., Wang, Y., Brindle, I. D., De Luca, V., and Després, C. (2012). The Arabidopsis NPR1 protein is a receptor for the plant defense hormone salicylic acid. Cell Reports **1**, 639-647.

Zeier, J. (2013). New insights into the regulation of plant immunity by amino acid metabolic pathways. Plant Cell Environ. **36**, 2085-2103.

Zeier, J., Pink, B., Mueller, M.J., and Berger S. (2004). Light conditions influence specific defense responses in incompatible plant–pathogen interactions: uncoupling systemic resistance from salicylic acid and PR-1 accumulation. Planta. **219**, 673-683.

Zhang, Z., Feechan, A., Pedersen, C., Newman, M.A., Qiu, J.L., Olesen, K.L., and Thordal-Christensen, H. (2007). A SNARE-protein has opposing functions in penetration resistance and defence signalling pathways. Plant J. **49**, 302-312.

Zhao, J., and Last, R.L. (1996). Coordinate regulation of the tryptophan biosynthetic pathway and indolic phytoalexin accumulation in Arabidopsis. Plant Cell. **8**, 2235-2244.

Zhao, Y., Hull, A.K., Gupta, N.R., Goss, K.A., Alonso, J., Ecker, J.R., Normanly, J., Chory, J., and Celenza J.L. (2002). Trp-dependent auxin biosynthesis in *Arabidopsis*: involvement of cytochrome P450s CYP79B2 and CYP79B3. Genes Dev. **16**, 3100-3112.

Zhou, N., Tootle, T.L., and Glazebrook, J. (1999). Arabidopsis *PAD3*, a gene required for camalexin biosynthesis, encodes a putative cytochrome P450 monooxygenase. Plant Cell. **11**, 2419-2428.

Table 1.

#	RT (min)	m/z	compound		abun-dance	Col-0 mock	Col-0 *Psm*	*79b2/3* mock	*79b2/3* *Psm*
						(mean ± SD)			
1	11.6	**86**, 59	n. i.		++	1.0 ± 0.2	17.9** ± 5.1	1.2 ± 0.4	3.5* ± 1.5
2	13.7	**117**, 90, 89	Indole[2]	C	++	1.0 ± 0.2	15.8** ± 4.1	0.7 ± 0.1	0.5 ± 0.2
3	15.3	131, **130**	Indole-3-carbinol (I3C)[1]	J	+	1.0 ± 0.1	2.3* ± 0.4	0.2 ± 0.1	0.2 ± 0.02
4	16.4	162, 144, **102**	n. i.		+	1.0 ± 0.5	31.9*** ± 0.9	0.4 ± 0.1	3.2* ± 0.9
5	17.0	**132**	n. i.		++	1.0 ± 0.4	5.1** ± 1.1	0.3 ± 0.1	0.3 ± 0.1
6	20.8	161, **130**	Indole-3-ethanole (Tryptophol)[2]	K	+	1.0 ± 0.4	5.5*** ± 0.1	n. d.	n. d.
7	21.4	189, **158**	n. i. (MS similar to 2-Methyl-indole-3-carboxylic acid[3])		+	1.0 ± 0.2	22.6*** ± 1.5	n. d.	n. d.
8	21.45	**155**, 130	Indole-3-acetonitrile (IAN)[2]	H	++	1.0 ± 0.3	1.5 ± 0.1	0.06 ± 0.01	0.06 ± 0.02
9	21.5	145, **144**, 116	Indole-3-carbaldehyde (ICC)[1]	E	++	1.0 ± 0.4	7.2** ± 1.7	0.4 ± 0.1	0.6 ± 0.2
10	21.6	**142**, 115, 88	Indole-3-carbonitrile (ICN)[2]	G	++	1.0 ± 0.6	26.8*** ± 3.7	1.1 ± 0.3	1.8 ± 0.6
11	22.1	175, **144**, 116	Indole-3-carboxylic acid (ICA)[1]	D	+++	1.0 ± 0.6	75.1*** ± 5.4	1.4 ± 0.4	1.6 ± 0.5
12	22.8	184, **158**	n. i.		+	1.0 ± 0.4	33.8** ± 8.1	n. d.	n. d.
13	23.7	**184**, 155, 129	n. i.		+	1.0 ± 0.4	93.5** ± 21.3	n. d.	n. d.
14	24.0	186, **171**, 143	4-Methoxy-indole-3-acetonitrile[2]	I	++	1.0 ± 0.1	1.9* ± 0.4	0.10 ± 0.01	0.11 ± 0.06
15	24.3	170, **144**, 116	n. i.		+++	1.0 ± 0.1	68.4** ± 16.1	0.7 ± 0.2	0.7 ± 0.3
16	24.4	**161**, 160, 104	n. i. (MS similar to 5-Hydroxy-indole-3-carbaldehyde[3])		+	1.0 ± 0.3	10.1*** ± 0.7	0.24 ± 0.11	0.26 ± 0.05
17	25.0	174, **130**	n. i.		++	1.0 ± 0.2	88.6** ± 18.9	0.7 ± 0.2	1.7 ± 0.5
18	26.0	191, **160**, 132	n. i. (MS similar to 5-Methoxy-tryptophol[3])		+	1.0 ± 0.4	46.3*** ± 6.8	0.7 ± 0.4	0.8 ± 0.3
19	26.4	**200**, 142, 115	Camalexin[1]	B	++++	1.0 ± 0.6	75.1*** ± 5.4	1.4 ± 0.4	1.6 ± 0.5
20	29.5	**271**, 229, 201	n. i.		+	1.0 ± 0.2	43.0*** ± 4.1	0.6 ± 0.2	1.1 ± 0.6
21	29.7	260, **201**, 142	n. i.		+	1.0 ± 0.2	99.7** ± 22.2	1.0 ± 0.3	0.7 ± 0.2
22	31.1	**189**	n. i.		++	1.0 ± 0.2	121.9** ± 33.8	1.2 ± 0.4	13.1* ± 5.7
	32.6	**412**, 351, 255	Stigmasterol		+++	1.0 ± 0.1	138.8*** ± 20.5	2.0 ± 0.5	95.5*** ± 8.7

Table 1. Indolic metabolite accumulation in *P. syringae* pv. *maculicola* (*Psm*)-inoculated leaves of soil-cultivated Arabidopsis Col-0 plants, as determined by comparative, GC/MS-based analyses of leaf extracts from wild-type Col-0 and the *cyp79b2/3* mutant impaired in Trp catabolism.

Leaves of the Col-0 wild-type and *cyp79b2/3* were inoculated with *Psm* or infiltrated with a $MgCl_2$-solution (mock-treatment), and harvested at 48 hpi for metabolite analyses. Analyses included leaf extraction, work-up, methylation of potentially existing free carboxylic groups in analytes, and GC/MS-based separation and detection. Comparison of individual ion chromatograms (m/z between 50 and 300) identified 22 peaks that significantly accumulated in extracts of *Psm*-inoculated Col-0 leaves but not in *cyp79b2/3*, and thus represent putative indolics. Many substances unrelated to the indole pathway significantly accumulated in both Col-0 and *cyp79b2/3* upon *Psm* inoculation (stigmasterol is listed in the bottom line as an example). Retention times (RT) and typical masses (m/z) in the mass spectra (MS) of the substance peaks are given.

Peak areas were related to the fresh weight of leaf samples and the area of the m/z 130 ion of the internal standard indole-3-propionic acid (IPA). Means and standard deviations (SD) from the resulting values were calculated and expressed relative to the mean value of the Col-0 mock-sample. The depicted values are based on at least three replicate samples per treatment and genotype. Asterisks denote statistically significant differences between $MgCl_2$- and *Psm*-treatments of each genotype ($^{***}P < 0.001$, $^{**}P < 0.01$, $^{*}P < 0.05$; two tailed *t* test). Plus signs indicate the range of the peak area values for the Col-0-*Psm* samples and thus yield estimates for the absolute amounts of accumulating substances in leaves (++++: very strong accumulation, mean peak area $> 2*10^8$; +++: strong, $2*10^7$-$2*10^8$; ++: medium, $2*10^6$-$2*10^7$; +: weak, $< 2*10^6$).

Substance identification was performed on basis of

[1]: comparison of RT and MS with those of authentic substances or

[2]: matching the MS with spectra of the NIST library.

[3]: MS of substance peaks showed similar but not identical mass spectra to the given compounds (n. i.: substance not identified).

FIGURE LEGENDS

Figure 1. Chemical structure of selected indolics.

(A) Tryptophan (Trp), (B) camalexin, (C) indole, (D) indole-3-carboxylic acid (ICA), (E) indole-3-carbaldehyde (ICC), (F) indol-3-ylmethylamine (I3A), (G) indole-3-carbonitrile (ICN), (H) indole-3-acetonitrile (IAN), (I) 4-Methoxy-IAN, (J) indole-3-carbinol (I3C); (K) tryptophol; (L) indol-3-ylmethylglucosinolate (I3M), (M) 4-Methoxy-I3M. The three indolics accumulating systemically in plants when leaf-inoculated with *P. syringae* are highlighted in grey.

Figure 2. Indole accumulation in *P. syringae*-inoculated (1°) and in non-inoculated, systemic leaf tissue (2°) of Arabidopsis Col-0 plants.

Levels of Trp, camalexin, ICA, ICC, I3A, and I3M in leaves of soil-cultivated Col-0 plants inoculated with *P. syringae* pv. *maculicola* (*Psm*) or infiltrated with a 10 mM $MgCl_2$ mock-control solution, are given in µg g^{-1} leaf fresh weight (FW). 1°: inoculated/treated leaves. 2°: leaves distal to inoculation/treatment. Leaf samples were harvested at 48 hours post inoculation (hpi). Data represent the mean ± SD of at least three replicate samples. Asterisks denote statistically significant differences between $MgCl_2$- and *Psm*-treatments ($^{***}P < 0.001$, $^{**}P < 0.01$, $^{*}P < 0.05$; two tailed *t* test).

Figure 3. Time course of indole accumulation in Col-0.

Time course of I3A, ICA, camalexin, and salicylic acid (SA) accumulation in leaves of soil-cultivated Col-0 plants inoculated with compatible *Psm* or hypersensitive response-inducing *Psm avrRpm1*. Endogenous levels of metabolites were determined in inoculated leaves at 6, 10, 24 and 48 hpi. Data represent the mean ± SD of at least three replicate samples. Hash symbols denote statistically significant differences between the $MgCl_2$ control treatment and the *Psm* or *Psm avrRpm1* inoculation at each time point ($^{###}P < 0.001$, $^{##}P < 0.01$, $^{#}P < 0.05$; two tailed *t* test).

Figure 4. *P. syringae*-inducible indole accumulation in mutants impaired in indolic metabolism at the site of inoculation.

Accumulation of Trp, I3A, ICA, ICC, and camalexin in Col-0, *cyp79b2/b3*, *pen2*, *myb34*, *myb51*, *myb122* and *myb34/51/122* (*tmyb*) in *Psm*-inoculated leaves of soil-cultivated plants. Endogenous levels of metabolites were determined at 48 hpi. Data represent the mean ± SD of at least three replicate samples. Asterisks denote statistically significant differences between $MgCl_2$ and *Psm* treatment in one genotype ($^{***}P < 0.001$, $^{**}P < 0.01$, $^{*}P < 0.05$; two tailed *t* test). Hash symbols denote statistically significant differences between the same treatment of Col-0 and the corresponding mutant ($^{\#\#\#}P < 0.001$, $^{\#\#}P < 0.01$, $^{\#}P < 0.05$; two tailed *t* test).

Figure 5. *P. syringae*-inducible indole accumulation in mutant plants affected in camalexin production.

Levels of **(A)** camalexin, **(B)** IAN, **(C)** I3A, and **(D)** ICA in *Psm*-inoculated and $MgCl_2$-infiltrated leaves of soil-cultivated Col-0, *cyp71A13*, *pad3*, *cyp81f1,* and *cyp81f2* plants at 48 hpi. Results from three independent biological experiments with Col-0 plants and different mutant combinations are depicted. Data represent the mean ± SD of at least three replicate samples. Compare legend to Fig. 4 for further details.

Figure 6. Impact of exogenous salicylic acid and pipecolic acid treatments on basal and inducible levels of indolics in leaves of Col-0 plants.

(A) Exogenous SA increases the basal und *Psm*-inducible levels of I3A at the expense of I3M. Please note the logarithmic scaling of the y-axes.

Three leaves of soil-grown Col-0 plants were first infiltrated with H_2O (light bars) or 0.5 mM SA solution (dark bars) (1^{st} infiltration/inf.). 4 hours later, the same leaves were subject to a second infiltration (2^{nd} inf.) with a 10 mM $MgCl_2$ (mock) solution or a suspension of *Psm.* For a third batch of plants, leaves were kept untreated (-) after the first infiltration. The leaves were harvested at the indicated times after the second treatment. Data represent the mean ± SD of three biological replicate leaf samples from different plants. Asterisks denote statistically significant differences between the respective H_2O and SA treatments ($^{***}P < 0.001$, $^{**}P < 0.01$, $^{*}P < 0.05$, ns: no significant differences; two tailed *t* test). Hash symbols above a *Psm*-sample indicate whether statistically significant differences exist between the secondarily mock- or *Psm*-treated samples that received the same first treatment. Analogously, hash symbols above a $MgCl_2$-sample indicate whether statistically significant

differences exist between the secondarily mock-treated and the untreated (-) samples ($^{###}P < 0.001$, $^{##}P < 0.01$, $^{#}P < 0.05$; two tailed *t* test).

(B) Exogenous Pip primes plants for enhanced *Psm*-triggered I3A and ICA accumulation.

Soil-grown Col-0 plants were supplied with 10 ml of 1 mM Pip (corresponsing to a dose of 10 µmol) or with 10 ml of H_2O (control treatment) via the root system. Leaves were challenge-inoculated with *Psm* or mock-infiltrated with 10 mM $MgCl_2$ one day later. Metabolite levels in leaves were determined 10 h after the challenge treatment. Values represent the mean ± SD of three biological replicates from different plants. Asterisks indicate whether statistically significant differences exist between the H_2O/*Psm*-samples and the Pip/*Psm*-samples ($^{***}P < 0.001$, $^{**}P < 0.01$, $^{*}P < 0.05$, ns: no significant differences; two tailed *t* test). Hash symbols indicate whether statistically significant differences exist between a given sample and the respective H_2O/mock-control samples ($^{###}P < 0.001$, $^{##}P < 0.01$, $^{#}P < 0.05$; two tailed *t* test).

Figure 7. *P. syringae*-inducible indole accumulation in mutants impaired in indolic metabolism in leaves distal from the inoculation site.

Levels of I3A, ICA, and ICC in Col-0, *cyp79b2/b3*, *cyp71A13*, *pen2*, *myb34*, *myb51*, *myb122,* and *myb34/51/122* (*tmyb*) in upper (2°) leaves after *Psm*-inoculation or $MgCl_2$-infiltration of lower (1°) leaves. Metabolite levels were determined at 48 hpi. Data represent the mean ± SD of at least three replicate samples. Asterisks denote statistically significant differences between $MgCl_2$ and *Psm* treatment in one genotype ($^{***}P < 0.001$, $^{**}P < 0.01$, $^{*}P < 0.05$, ns: no significant differences; two tailed *t* test). Hash symbols denote statistically differences between the same treatment of Col-0 and the corresponding mutant ($^{###}P < 0.001$, $^{##}P < 0.01$, $^{#}P < 0.05$; two tailed *t* test).

Figure 8. Levels of indolic metabolites in leaves of SAR-deficient mutant plants following *P.syringae* inoculation.

Levels of I3A, ICA and ICC in soil-grown Col-0, Pip-deficient *ald1*, *fmo1*, SA-deficient *sid2*, and *npr1* in **(A)** 2° leaves distal to the inoculation site and **(B)** in 1°, *Psm*-inoculated leaves. Levels of metabolites were determined at 48 hpi. A $MgCl_2$-infiltration of 1° leaves served as the mock-control treatment. Data represent the mean ± SD of at least three replicate samples.

Two independent experiments, one comprising Col-0, *ald1*, *fmo1*, and *sid2*, and one involving Col-0 and *npr1*, are shown. Compare legend to Fig. 6 for further details.

Figure 9. Pre-induced immunity of soil-grown *cyp79b2/3* and *pen2* plants dampens *P. syringae*-triggered SAR.

(A) SAR assays using soil-grown (left) and hydroponically-cultivated (right) Col-0, *cyp79b2/b3* and *pen2* plants. Lower (1°) leaves were infiltrated with either 10 mM $MgCl_2$ or inoculated with *Psm* to induce SAR. Two days later, three upper (2°) leaves were challenge-infected with *Psm*. Bacterial growth in upper leaves was determined 60 h post 2° leaf-inoculation. Data represent the mean ± SD of at least seven replicate samples. Asterisks denote statistically significant differences between *Psm*-pre-treated and mock-control samples ($^{***}P < 0.001$, $^{**}P < 0.01$, $^{*}P < 0.05$, ns: not significant; two tailed *t* test). Hash symbols denote statistically significant differences between the same treatment of Col-0 and the corresponding mutant within one cultivation system ($^{###}P < 0.001$, $^{##}P < 0.01$, $^{#}P < 0.05$; two tailed *t* test).

(B) Basal resistance assay in Col-0, *cyp79b2/b3* and *pen2* with soil-grown plants and plants cultivated in a hydroponic system. Full-grown leaves of naïve plants were inoculated with *Psm*, and bacterial growth was assessed 60 h later. Data represent the mean ± SD of at least seven replicate samples. See (A) for further details.

(C) Levels of SA in distal, 2° leaves upon *Psm*-inoculation of 1° leaves of soil- and hydroponically-cultivated Col-0, *cyp79b2/b3* and *pen2* plants at 48 hpi. $MgCl_2$-infiltration of 1° leaves served as the mock-control treatment. Data represent the mean ± SD of at least three replicate samples. Details as described in the legend to Fig. 7.

Figure 10. Soil-grown *myb34*, *myb51*, *myb122*, *myb51 myb122*, and *tmyb* plants display normal SAR.

SAR assay with soil grown Col-0, *myb34*, *myb51*, *myb122*, *myb51 myb122,* and *myb34/51/122* (*tmyb*) plants, as described in the legend of Fig. 9A.

Figure 11. Regulation of induced indolic metabolism in *P. syringae*-inoculated leaves, and possible consequences of dysfunctional, indole-related early immune layers on basal resistance and SAR.

(A) Simplified scheme of Trp-derived indolic metabolism in Arabidopsis and its activation in *P. syringae*-inoculated leaves. The general pathway is depicted in grey. Small up (down) arrows symbolize gene up- (down-) regulation upon bacterial inoculation (see Table S1). Metabolites determined in leaf extracts in this study are illustrated in black. The number of plus signs in brackets symbolises the quantity of *Psm*-induced indole accumulation in inoculated Col-0 leaves (see legend). The coloured squares next to or below the assessed metabolites symbolise the levels of these metabolites compared to wild-type Col-0 in *Psm*-inoculated leaves of mutant plants (see legend for details). Only mutants with accumulation patterns markedly differing from the wild-type are depicted for a particular metabolite (abbreviations: *79b2/3 = cyp79b2/3*, *71A13 = cyp71A13*, *81f1 = cyp81f1*, *81f2 = cyp81f2*). The levels of indoles in leaves of mutant plants reflect the influences of the functional genes on (*Psm*-induced) indolic metabolism. Note that, besides the biosynthetic pathway genes *CYP79B2/3*, *CYP71A13* and *PAD3*, *CYP81F1, CYP81F2*, and *MYB122* positively regulate camalexin production. Functional *CYP71A13*, *CYP81F1,* and *CYP81F2* negatively affect I3A, IAN, ICA, and ICC levels. I3A formation is positively regulated by *PEN2*, *MYB51*, and *MYB34*, and a *PEN2*-independent mode for I3A production exists. ICA and ICC formation is also stimulated by the action of *PEN2*. Trp catabolism is incapacitated if CYP79B2 and CYP79B3 are defective, leading to Trp over-accumulation. Exogenous SA stimulates I3M to I3A conversion. Exogenous Pip primes plants for enhanced *Psm*-triggered accumulation of I3A, camalexin, and ICA.

(B) Soil cultivation-dependent pre-induced immunity in *cyp79b2/3* and *pen2* masks *P. syringae*-triggered SAR. In the Col-0 wild-type, early pre-invasion immune layers, involving indole glucosinolate hydrolysis products such as I3A, are intact. Post-invasion, inducible immune layers are not activated. These naïve plants are able to induce a strong SAR response upon *P. syringae* attack of leaves. In *cyp79b2/3* and *pen2*, indole metabolism and early immune layers are weakened, and a soil cultivation-dependent factor induces enhanced basal resistance and SA accumulation. In these non-naïve plants with pre-induced immunity, a further resistance increase by SAR-inducing *P. syringae* is low or absent.

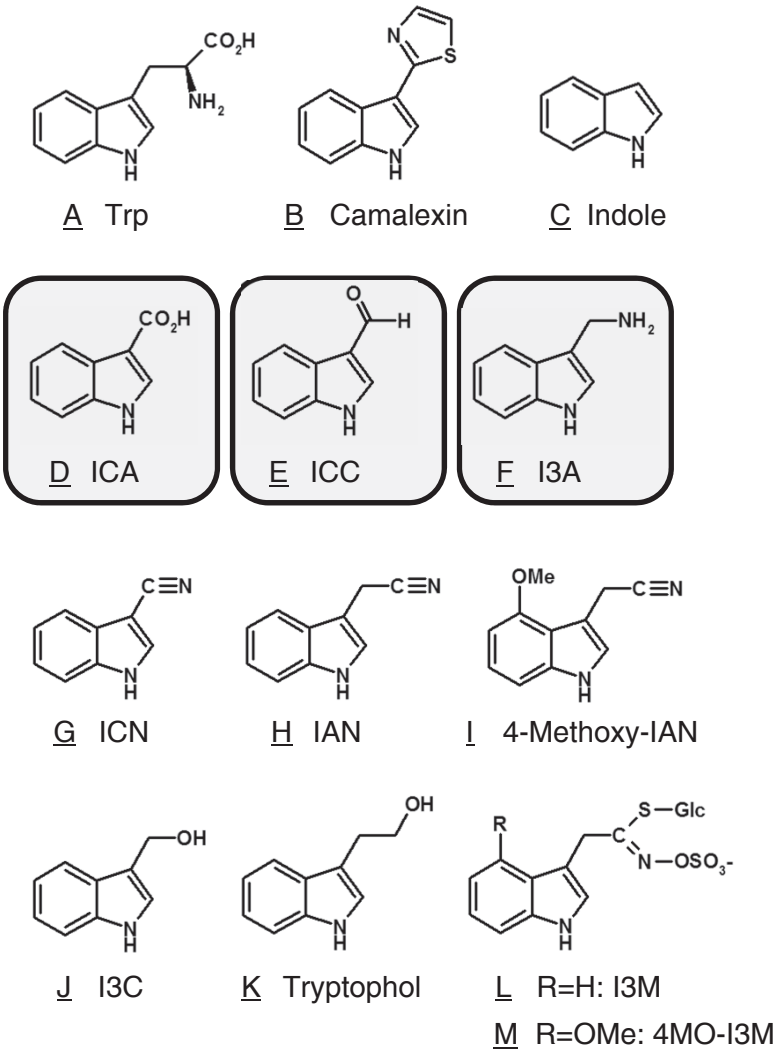

Fig. 1

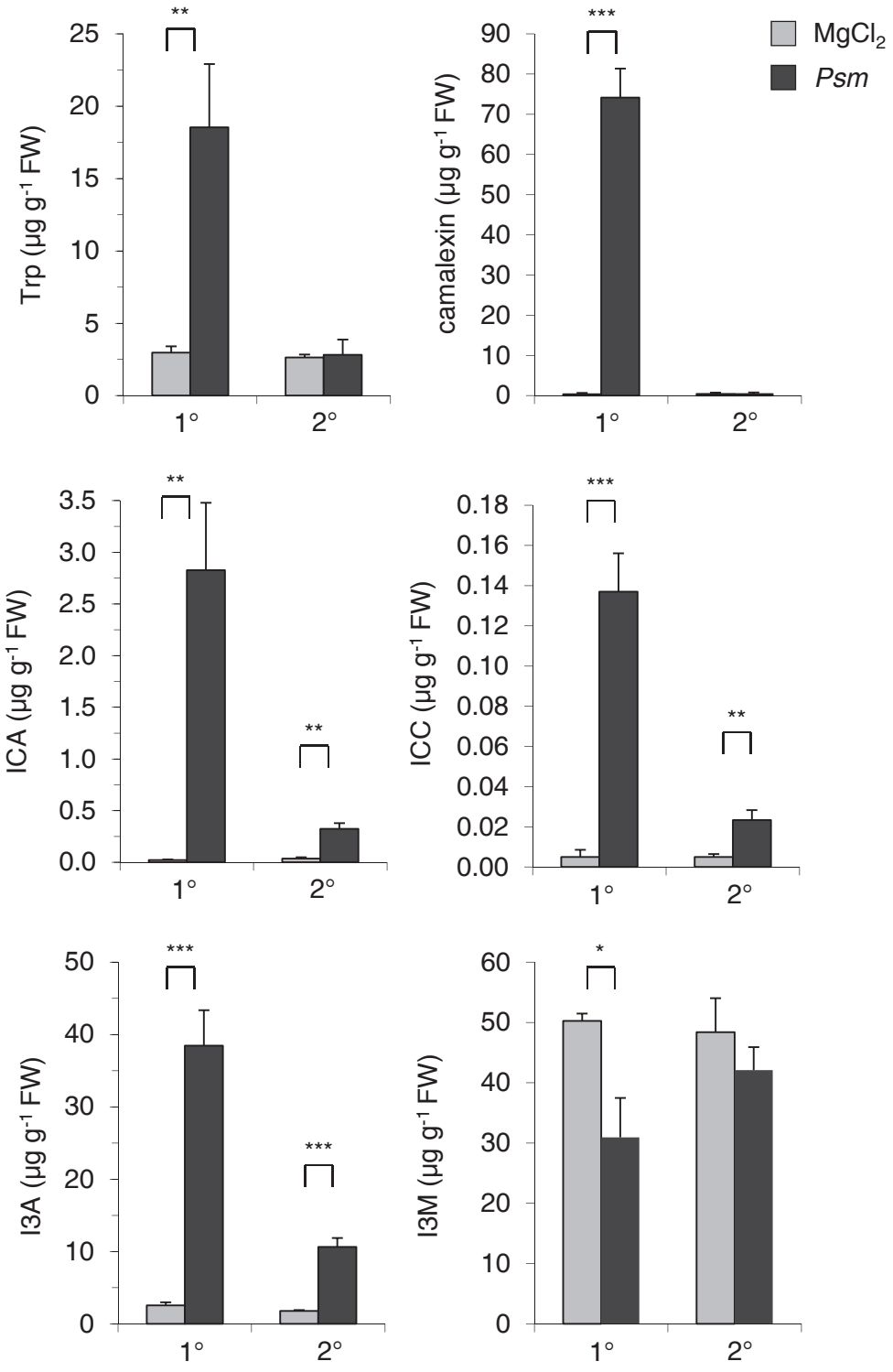

Fig. 2

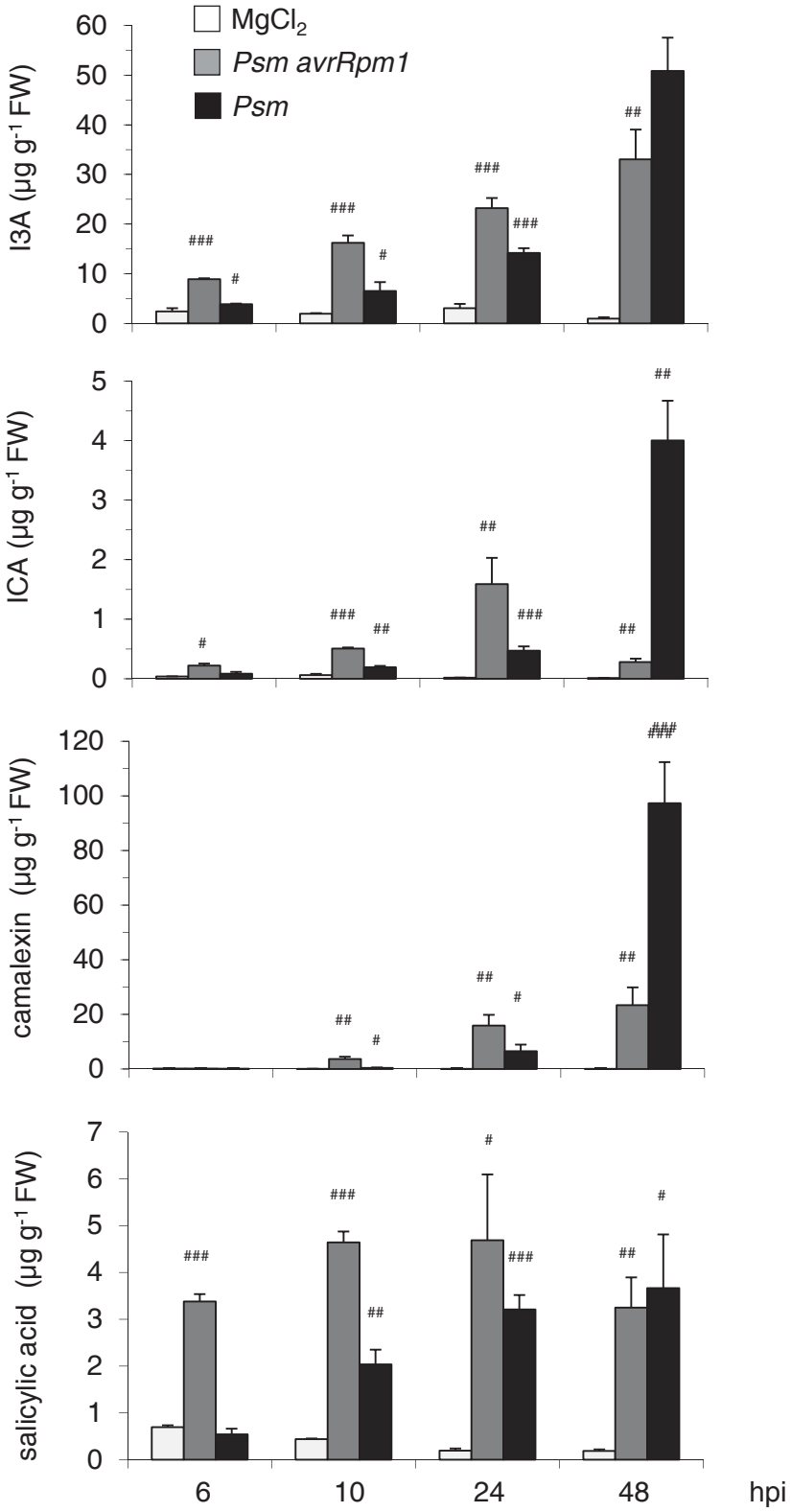

Fig. 3

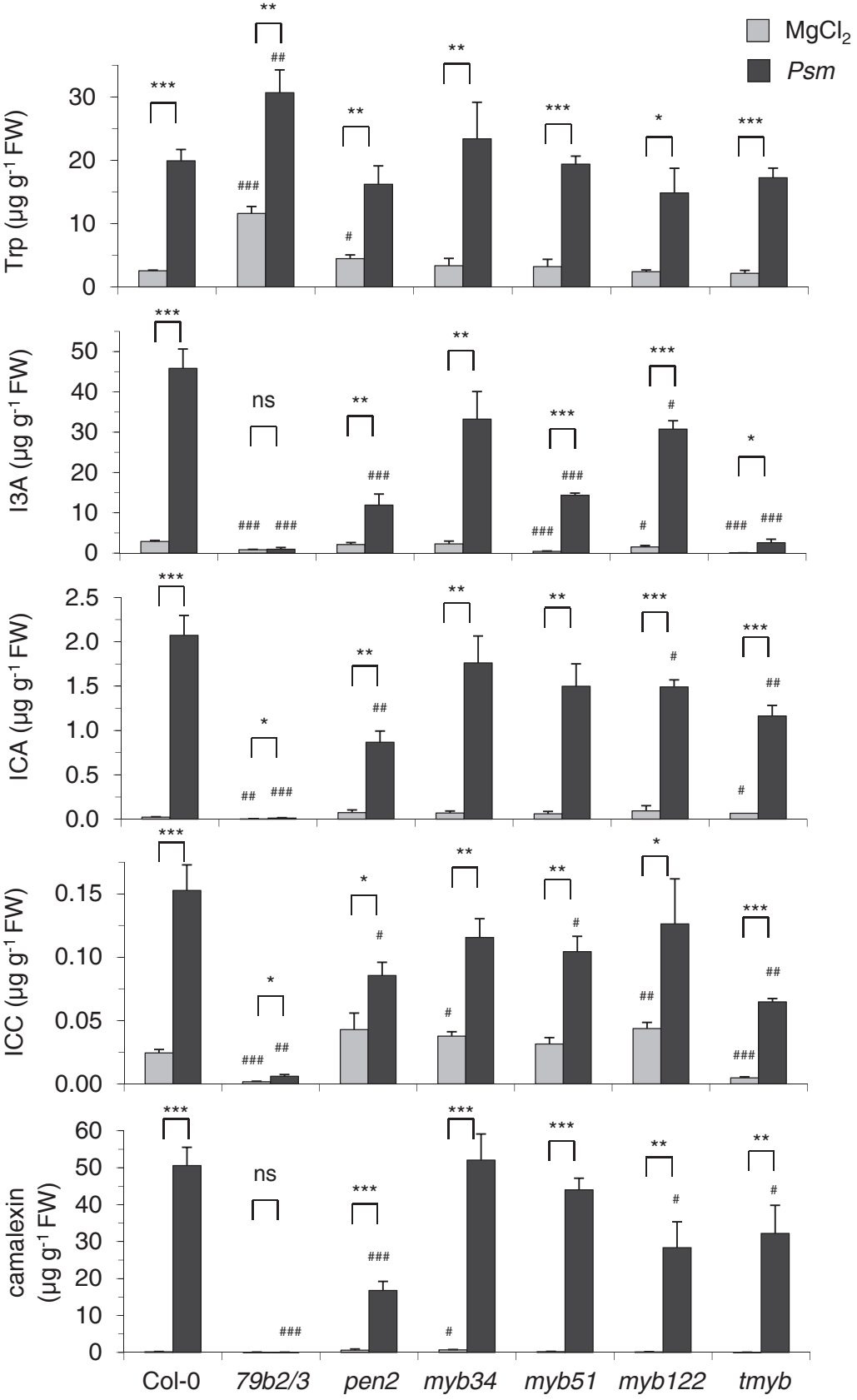

Fig. 4

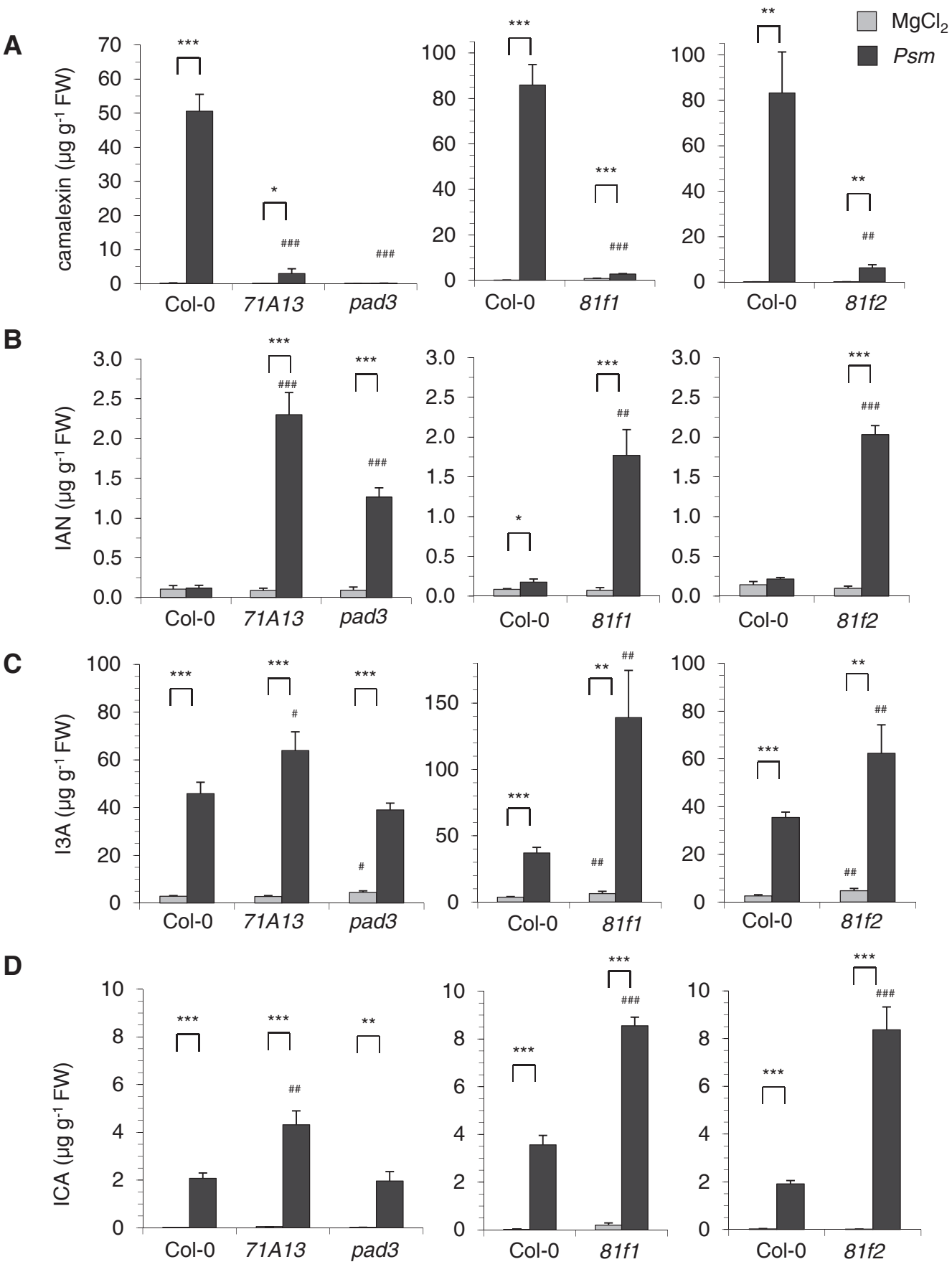

Fig. 5

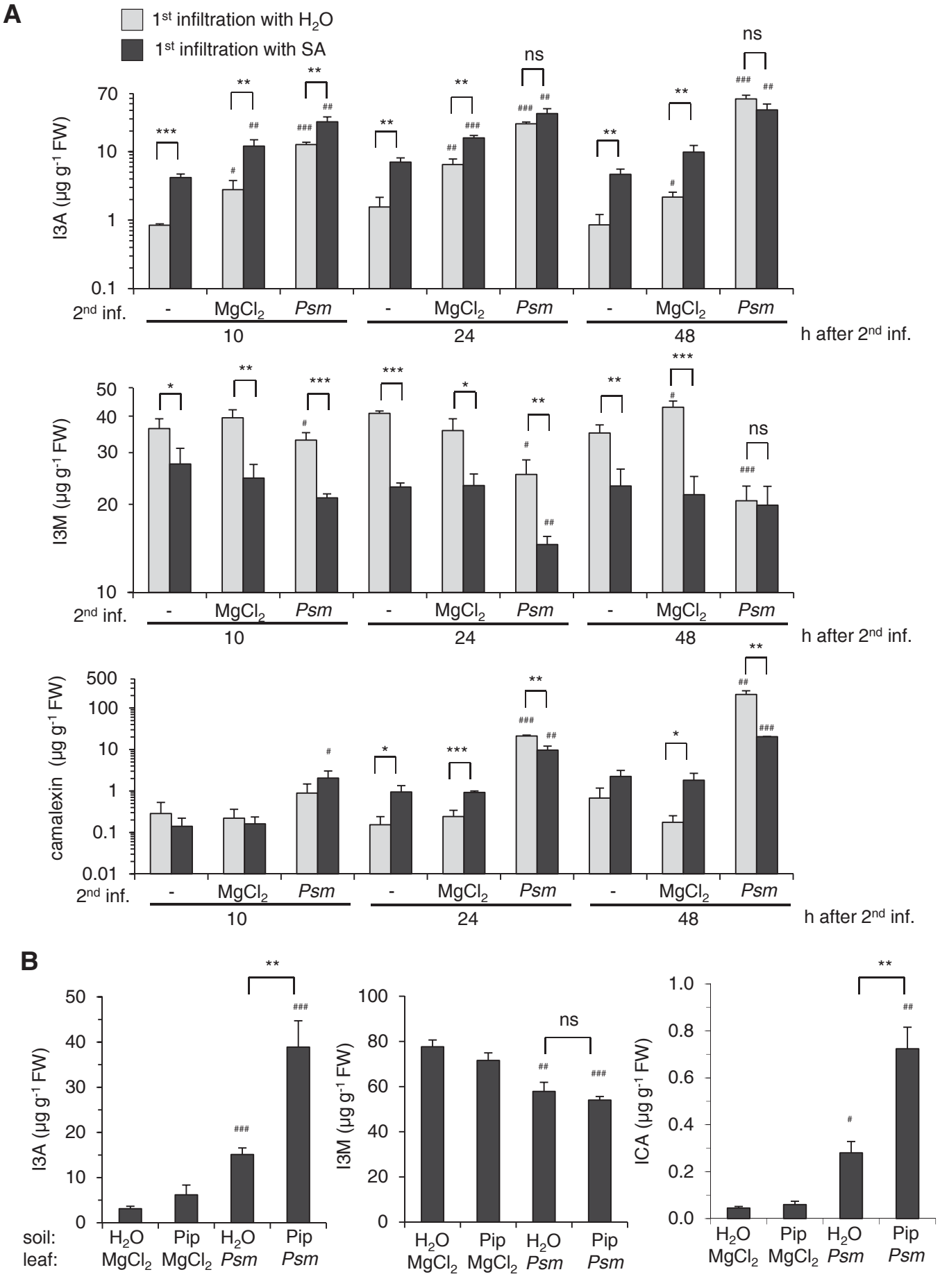

Fig. 6

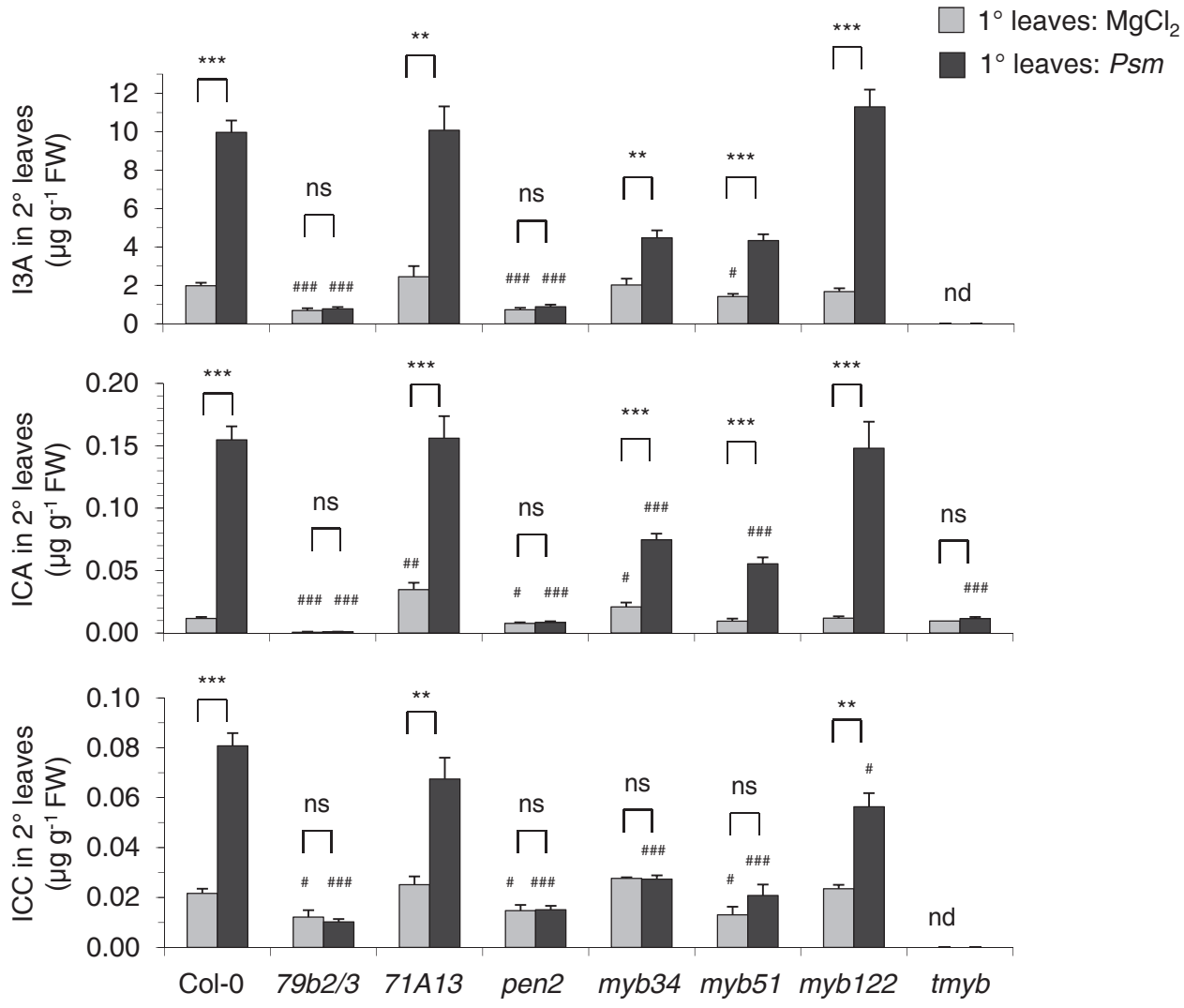

Fig. 7

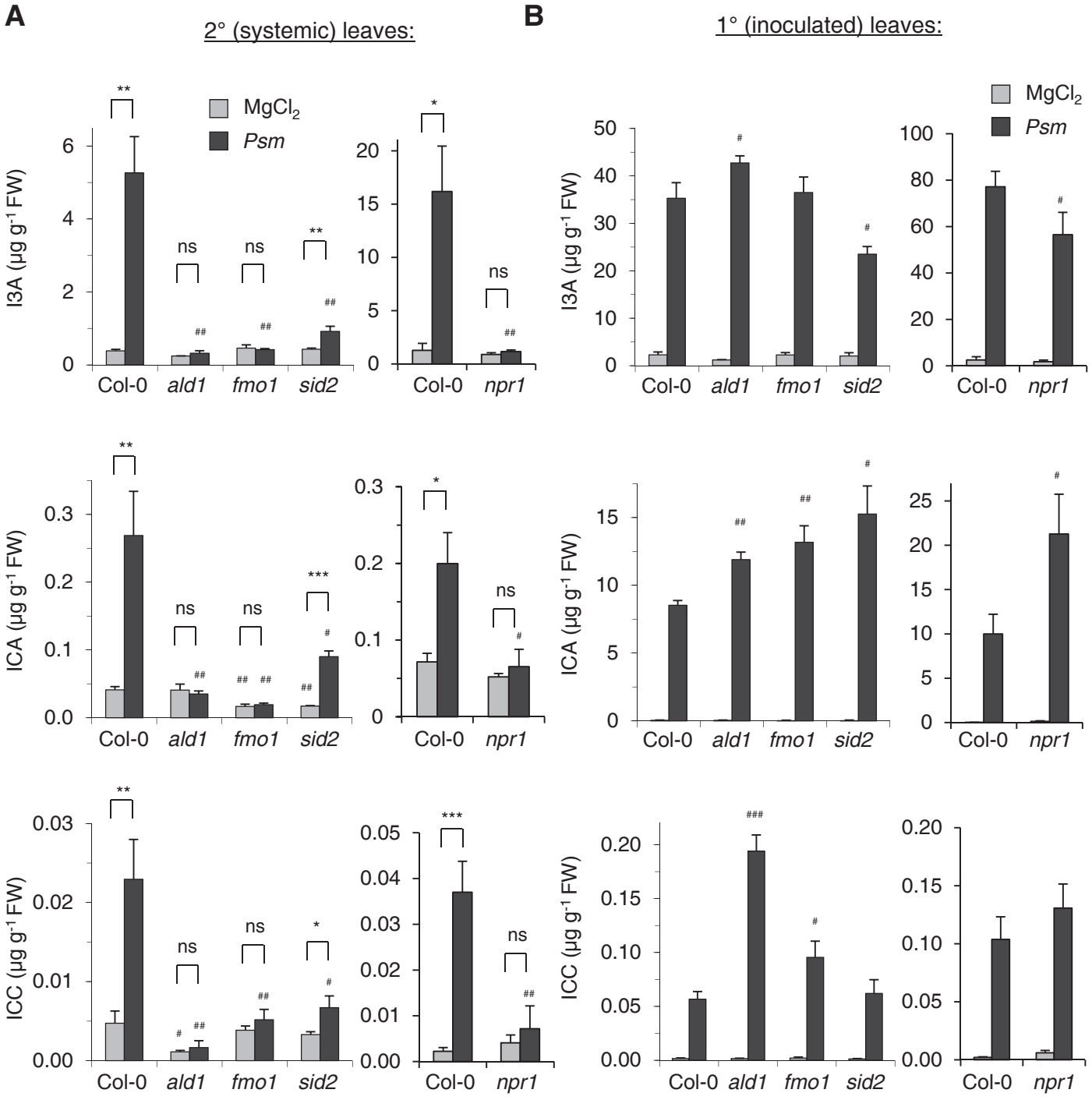

Fig. 8

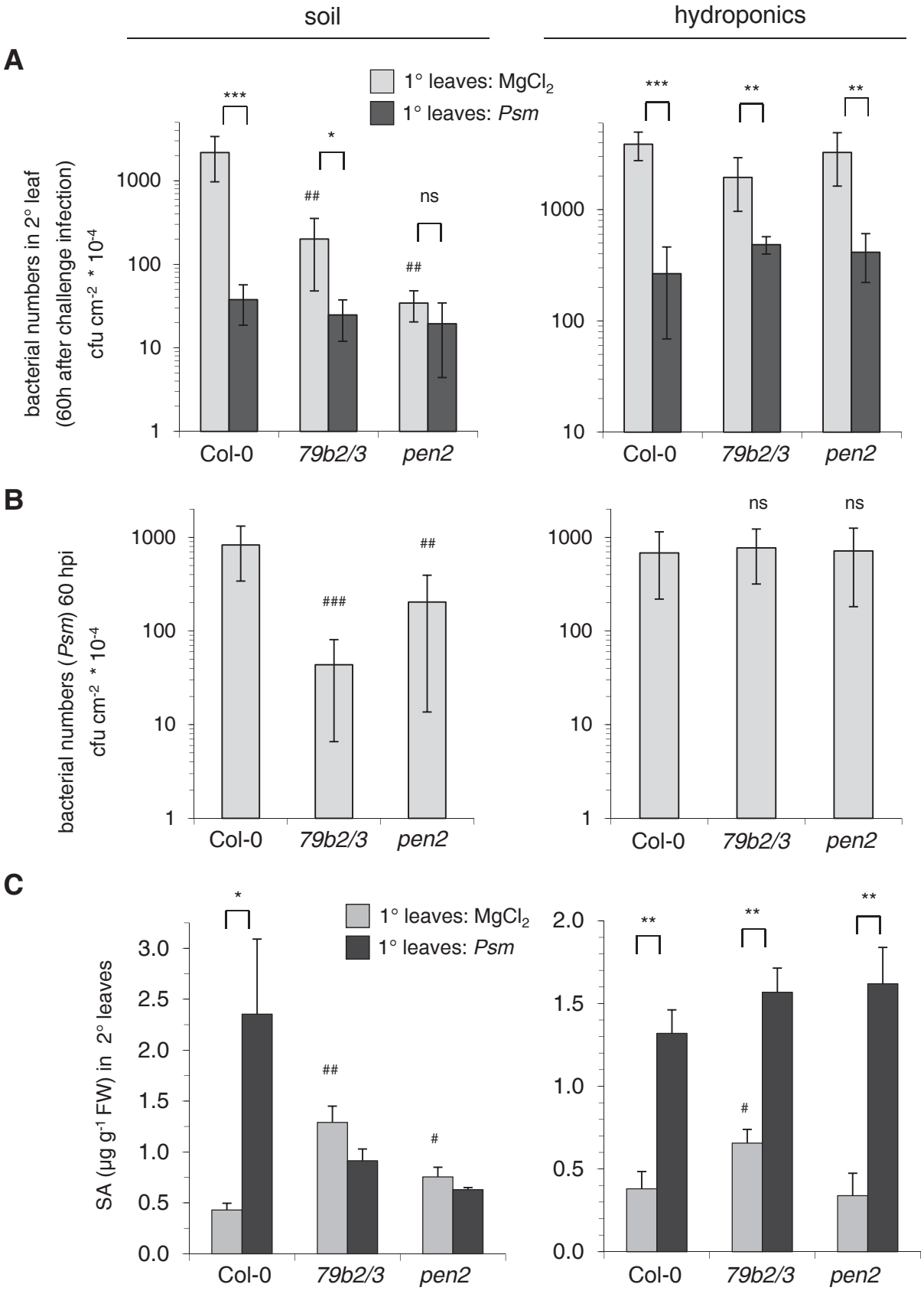

Fig. 9

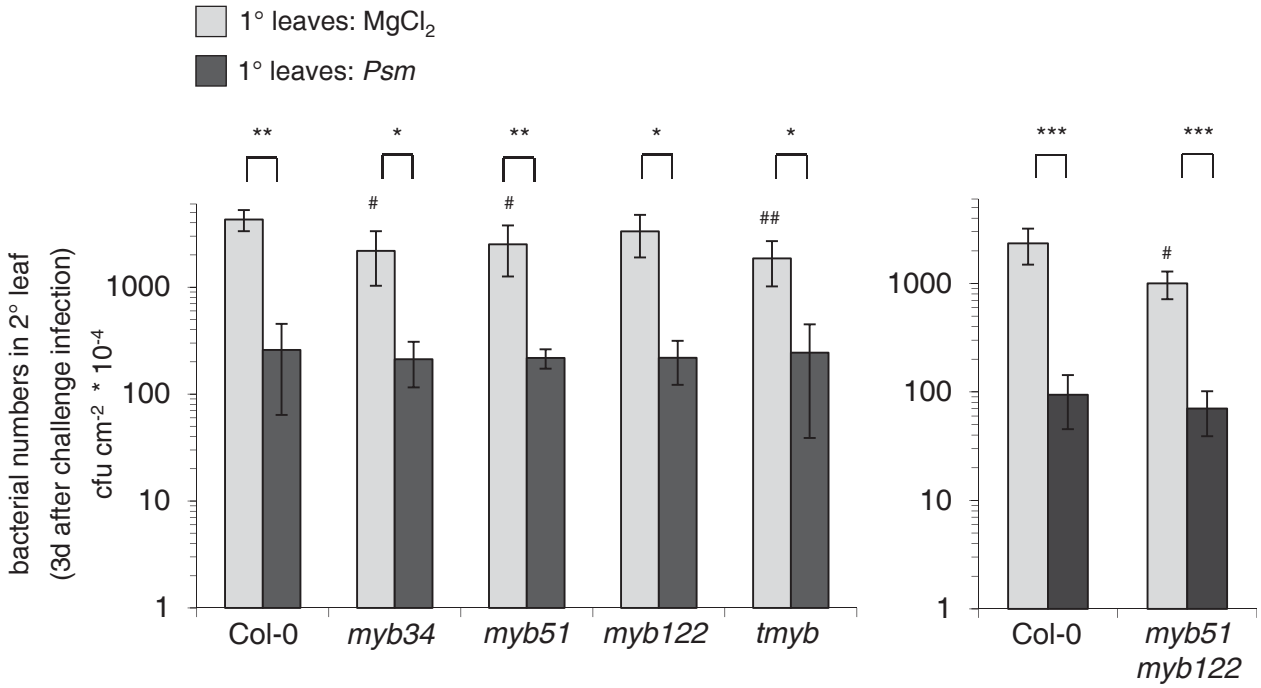

Fig. 10

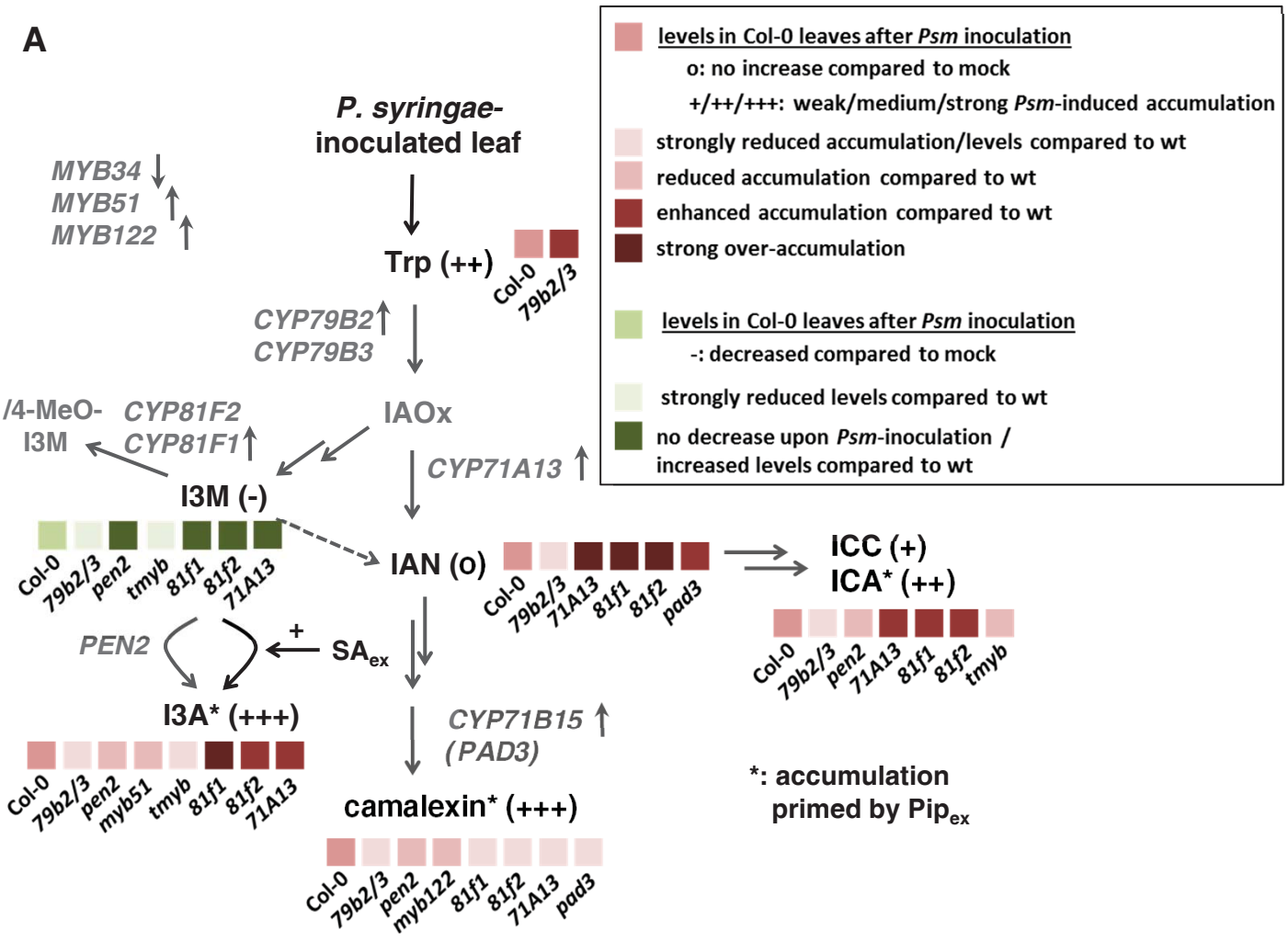

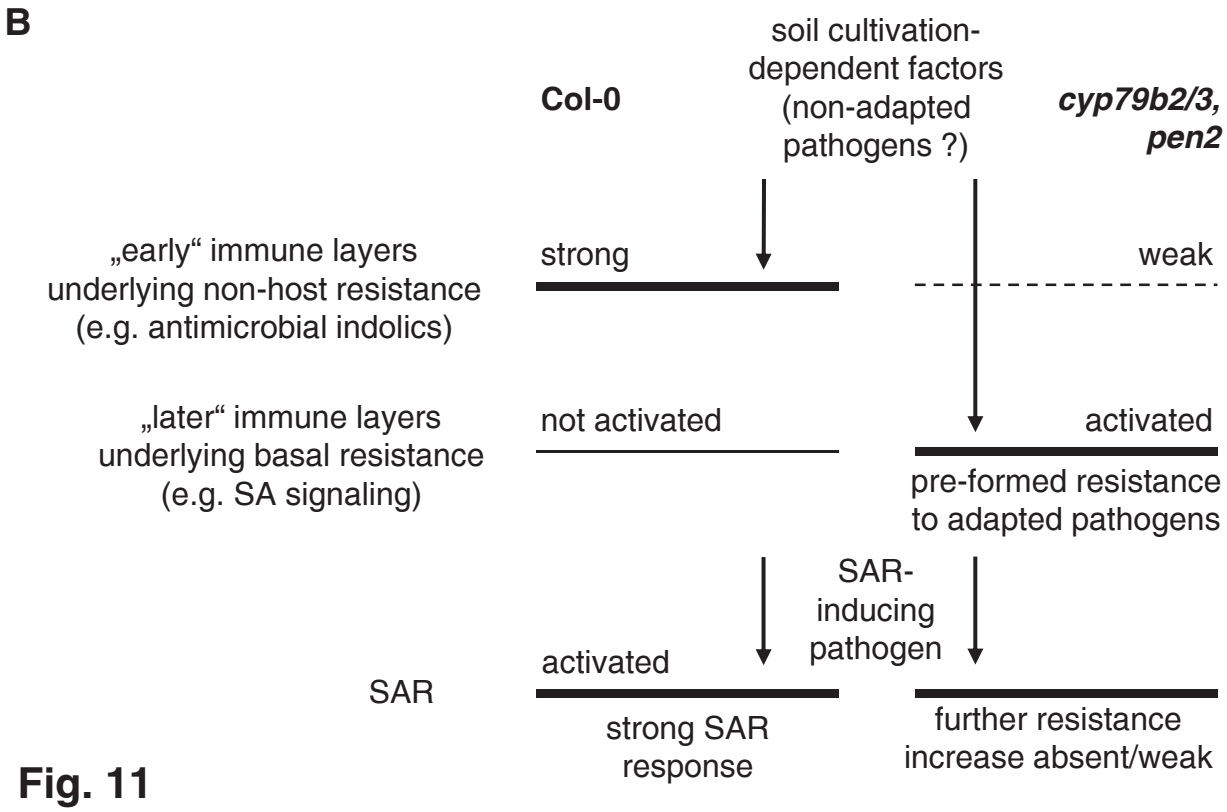

Fig. 11